Studies on Reactive Water-Dispersible Polyisocyanate and Polyurethane-Urea Micelle as Coating Materials

Tsutomu TAWA

2008

Contents

Chapter 1

General Introduction

1.1. Backgoroud

Polyurethane (PU) is a common polymer which is widely used in various fields such as fibers, elastomers, foams, coatings, and adhesives. The term "polyurethane" refers to the polymer which contains a significant number of urethane groups, regardless of what the rest of the molecule is.[1] PU is usually synthesized by the reaction of di- or poly- functional hydroxyl compounds with di- or poly- functional isocyanates. The general structure of a linear PU derived from a dihydroxyl compound, HO-R-OH, and a diisocyanate, OCN-R'-NCO, can be represented by the following formula:

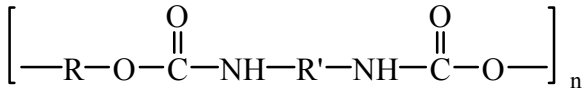

The structural changes can be made at will. Figure 1-1 shows the examples of usable compounds to prepare PU. A lot of hydroxyl-containing compounds (R) which are different in molecular weights and types (polyether, polyester, polycarbonate and simple glycols) can be used. Similarly, the structure of isocaynate (R') such as aromatic, alicyclic and aliphatic is also selective; consequently the combination of R and R' is innumerable. In addition, the increase of the functionality of the hydroxyl unit as well as the isocyanate yields branched or cross-linked polymers. The diversities of PU meet a lot of demands on practical uses and PU has been applied to the various fields. [2-5]

The chemistry of organic isocyanate, which is one of the important compounds consisting of PU, dates back over a hundred years. In 1849, Wurtz was the first to synthesize aliphatic isocyanates by reacting organic sulfates with cyanates: [6]

Hydroxyl-containing Compounds (R)

Simple Glycol

EG (Ethylene glycol)

NPG (2,2-Dimethyl-1,3-propanediol)

1,6-HD (1,6-Hexanediol)

TMP (1,1,1-Tris(hydroxymethyl)propane)

Gly (Glycerol)

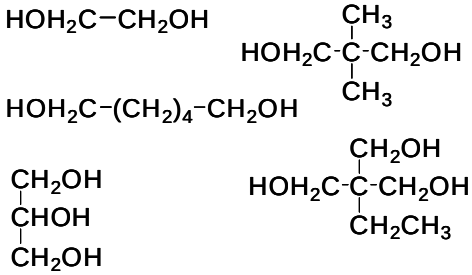

Polymer with hydroxyl Group

PPG (Poly(propylene glycol))

PTMG (Poly(tetrahydrofuran))

Polyester Polyol

PC (Polycarbonatediol)

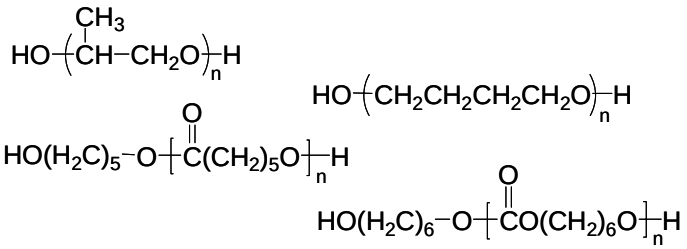

Isocyanate (R')

Aromatic

TDI (Tolylene Diisocyanate)

2,4-TDI

2,6-TDI

MDI (Methylenediphenyl 4,4'-Diisocyanate)

Alliphatic

HDI (1,6-Hexamethylene Diisocyanate)

Alicyclic

H6XDI (1,3-Bisisocyanatomethylcyclohexane)

IPDI (3-Isocyanatomethyl-3,5,5-trimethylcyclohexyl Isocyanate)

H12MDI (4,4'-Dicyclohexylmethanediisocyanate)

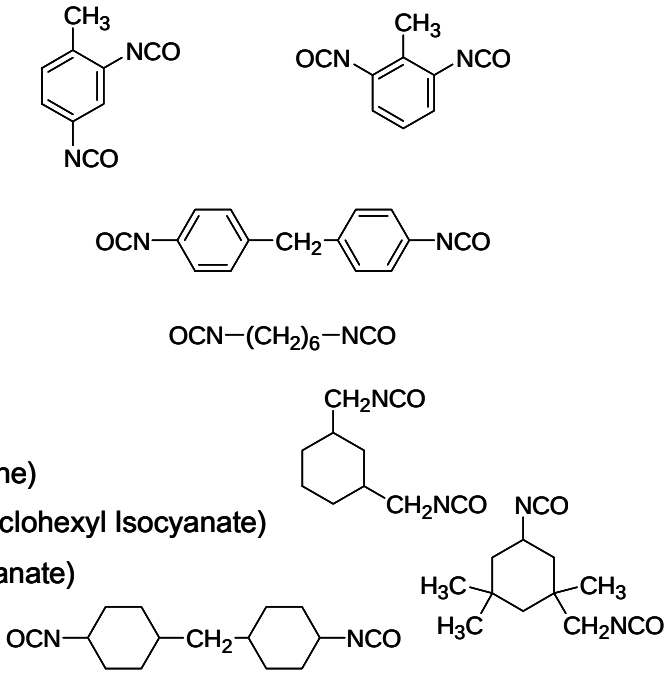

Figure 1-1. Usable compounds to prepare PU.

$$R_2SO_4 + 2KCNO \longrightarrow 2RNCO + K_2SO_4$$

The structure of the isocyanates obtained by Wurtz was later confirmed by Gautier. [7] Wurtz also observed several of the simple reactions of isocyanates, which are important commercially, today. The first aromatic isocyanate, phenyl isocyanate, was prepared by Hofmann [8] by pyrolysis of symmetrical diphenyl oxamide:

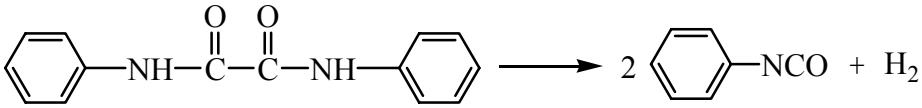

Among the many methods developed for the synthesis of organic isocyanates, that of Hentschel [9] is used in the production at present. It is based on the reaction of amines with phosgene:

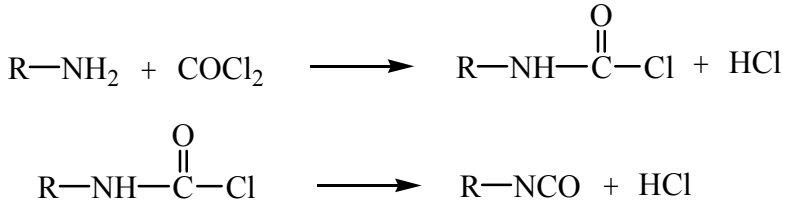

In the years following the research of Wurtz and Hentschel, many isocyanates were prepared and their simple reactions were characterized. It was not until approximately 1937, however, that the use of diisocyanates for polymer synthesis was explored. In 1937, Otto Bayer and co-workers [10] discovered the diisocyanate addition polymerization that resulted in the preparation of many different types of PUs. The reaction of hexamethylene diisocyanate with simple glycols such as 1,4-buthane diol led to the formation of PUs possessing characteristic properties as plastics and fibers. These PUs found commercial use under the trade name of Igamid U for plastics and Perlon U for

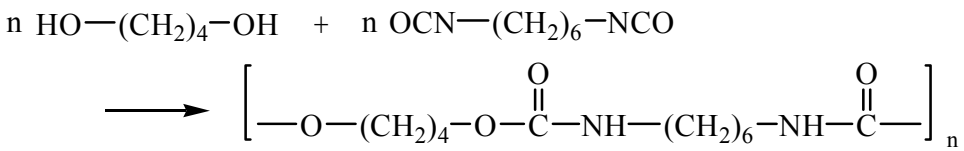

synthetic fibers.

The development of PUs in fields other than plastics and fibers was actively pursued in the 1940s. In 1940, Schlack [11] reacted polyesters containing terminal hydroxyl groups with HDI and prepared the products with very low softening temperatures. This is the first time to introduce polymer glycol to prepare PU, and extensive researches after that have generated promising uses in various fields such as rigid or flexible foams [12, 13], elastomers [14, 15], adhesives [4, 16] and coatings.[17, 18]

PU coating is one of the earliest fields to be investigated among many commercial applications. Bayer and co-workers developed polyester-diisocyanate coatings (Desmodur-Desmophen combinations), which were two-component (2K) system based on the formation of urethane groups by the reaction of the hydroxyl groups of polyesters with the isocyanate groups. PU coatings were found to be eminently suitable for various substrates such as wood, rubber, paper, plastic film, and metal, because they have made it possible to obtain a wide variety of properties ranging from very flexible to hard and brittle films by varying the type and the degree of branching of polyester and diisocyanate, as well as the NCO / OH ratio. They have also achieved some outstanding characteristics such as high gloss, excellent water and solvent resistance, and good weather stability. However, 2K system was very sensitive to the work environment, since free NCO groups were so reactive that they brought out the side reaction with water molecules including in organic solvent and the moisture. It has an inevitably limited usable time so-called “pot life”.

The efforts for improving handling have facilitated to develop one-component (1K) system; PU with high molecular weight is coated on a substrate from the solution so-called “polyurethane lacquer” and the solid film is formed by the evaporation of

solvent.[19, 20] It has strong points such as storage stability and ease of application, but cannot achieve performances such as heat resistance and hardness because PU consisting of 1K system is a thermoplastic polymer.

Recently, the public concern on environment has been increasing and the emission regulation of volatile organic compounds (VOCs) has been strict year by year. These regulations and social demands drive industries to develop environmentally friendly products. [21-24] Under the social background, organic solvent based PUs have been restricted in coating systems. Among several options to reduce or eliminate organic solvents, water is the best choice to use as a medium, and therefore, aqueous polyurethane dispersion (PUD) has received considerable attention.

Several processes have been developed for the synthesis of PUD. PUs are basically hydrophobic, so that emulsifiers are needed to disperse them into water. PUD is classified into two major classes of using either external or internal emulsifiers. The first isocyanate based aqueous dispersion was developed by Schlack in 1943, [25] which was the type of using external emulsifiers. It was prepared by the reaction between a diisocyanate dispersed in water by the emulsifier and an equivalent amount of a diamine under vigorous stirring. Further researches have produced a lot of PUDs suitable for coating textile or leather. [26] However, they had usually lager particle sizes (ca. 1 μm), resulting in instability. More advantageous is the introduction of internal emulsifiers into the polyurethane backborne. The hydrophilic groups can be incorporated during the synthesis of PUDs. PUDs with internal emulsifiers are divided into three types in ionic character of hydrophilic groups; cationic, [27-29] non-ionic, [30] and anionic. Among them, the anionic type PUD is the most common. Anonic PUDs can be prepared from polyols containing carboxylic acid [31-49] and sulfonic acid groups. [50] The varieties of PUD

preparation methods have contributed to the development of waterborne one-component polyurethane (WB 1K-PU) system. [51-53] However, there were also two deficiencies due to mainly thermoplastic polymer as well as solvent based 1K system: heat resistance and hardness.

Considering the performance of solvent based PU, it stands to reason that the WB 2K-PU system has been widely introduced since the 1990 when water-dispersible polyisocyanate (WDPI) was developed by modifying polyisocyanate with hydrophilic methoxy polyethylene glycol (MPEG). The standard of WB 2K-PU system is the combination of aqueous polymer dispersion with hydroxyl unit and WDPI. [54-61] These components are easily mixed by stirring and form a stable aqueous dispersion with a low viscosity. It allowed to achieve both the performance of solvent based 2K-PU system and the reduction of VOCs. Although the large advantage of the WB 2K-PU system has put it to practical use in the last decade, there are only very few reports on the fundamental analysis.

PU is a polymer with both the soft and hard segments in one molecule. The soft and hard segments are formed by polymer glycol and the urethane linkage of diisocyanate and simple glycols, respectively. [62, 63] Because of the cohesive force between hard segments, PU undergoes microphase separation into soft- and hard-segment domains as shown in Figure 1-2. The intrinsic structure of PU has been subjected to study for more than 50 years. [64-71] As mentioned above, PUD can be prepared by introducing ionic moieties into a PU chain and the presence of an ionic group in the hard segment has a considerable effect on its physical properties. [43, 47, 49, 72, 73]

According to calculations by Salame, [74, 75] hydoroxyl and amide groups are effective on exhibiting gas barrier property, because intermolecular cohesions increased

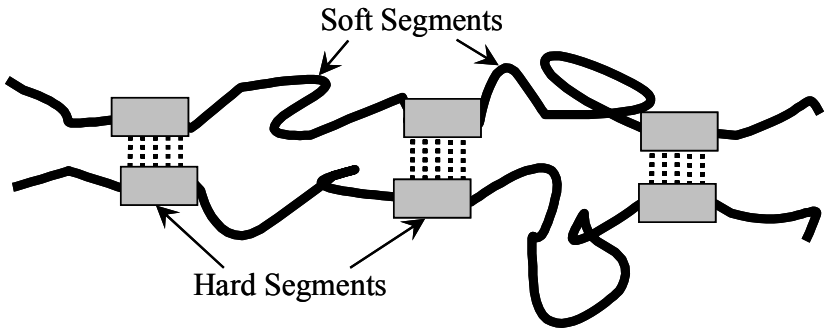

Figure 1-2. Structure of PU Chain.

by hydrogen boding retard gas permeation. Conventional PU is gas permeable polymer, because it contains considerable amount of soft segments and the soft domains work as the pathway of gas. Because urethane and urea groups in PU have high cohesion energy due to their hydrogen bondings, the well-designed PU with extremely high concentration of urethane and urea groups is expected to be a novel type polymer with gas barrier property.

In order to enhance further gas barrier performance, platelike flakes dispersed into polymer matrix are effective, because the permeable molecules have to wiggle around them and move through a tortuous pathway.[76-86] Platelike nanoflakes are ideal due to their geometrical shape and high aspect ratio. Montmorillonite (MMT) is a representative material, but there are only a few studies about the permeation-barrier properties of PU and MMT composites,[87-90] especially quite a few about PUD.

1.2. Outline of This Thesis

The objective of this thesis is to clarify the characteristics and properties of aqueous PU in solution and in films as PU coating. The compound of two types in aqueous PU, WDPI and PUD, are targets; WDPI is an oligomer containing active NCO groups, and

PUD is a polymer with extremely small amount of OH or amine groups in the end. On WDPI, the structural change with the reaction is mainly discussed. For PUD, the role of hard segment is clarified by the systematic study using prepared PUDs with different concentrations of hard segment.

This thesis consists of six chapters. The first chapter describes the background of polyurethane coatings and the subjects of the investigation. The following chapters are divided into two parts.

Part I (Chapters 2-4) is concerned with the WDPI. In Chapter 2, a novel type WDPI is prepared by hexamethylene diisocyanate allophanate (HDI) modified with methoxy polyethylene glycol (MPEG). It has a character of excellent water dispersibility due to the extremely low viscosity. The NCO units of WDPI show a characteristic reaction with an induction period in water medium. The relation between the characteristic reaction and the micelle structure of WDPI is discussed. In Chapter 3, it is focused on the structure inside the WDPI micelle. The progress of reaction and structural changes are probed by the microviscosity inside the micelle, which is quantitatively estimated from two fluorescence techniques: the excimer formation rate and the fluorescence depolarization. The change of microviscosity of WDPI with the reaction in water medium is studied in detail. In Chapter 4, WB 2K-PU system consisting of PUD and WDPI is subject on research. In WB 2K-PU system, intermicellar reaction between PUD and WDPI proceeds in colloidal state. The structural change of the obtained film with the reaction and the effect of film structure on the mechanical properties are studied.

In Part II (Chapters 5 and 6), the role of hard segment in PUD is clarified from the molecular side. In Chapter 5, some series of PUDs are prepared with the difference in

fraction and intra-chain distance of hard segments, amount of ionic COOH group and type of counter-ion. By using these PUDs, the role of hard segments on the structure and mechanical properties of resulting film is clarified. In Chapter 6, a novel type PUD consisting of only hard segments is prepared. The PUD offers a high oxygen barrier performance. In order to improve the oxygen barrier performance, it is an effective method to distribute inorganic compounds like MMT in a polymer matrix. The composite of the new PUD and MMT shows predominant oxygen barrier property. The chemical structure of hard segment and the distribution of MMT in PU matrix are investigated for attaining high gas barrier performance.

References

1. J. H. Saunders and K. C. Frisch, "*Polyurethanes, Part I, Chemistry*", Interscience, New York (1962)
2. M. F. Sonnenschein, N. Rondan, B. L. Wendt, and J. M. Cox, *J. Polym. Sci. Part A: Polym. Chem.,* **42**, 271 (2004)
3. W. Tang, R. J. Farries, W. J. Macknight, and C. D. Eisenbach, *Macromolecules*, **27**, 2814 (1994)
4. T. K. Chen, Y. I. Tien, and K. H. Wei, *Polymer*, **41**, 1345 (2000)
5. G. Consolati, M. Levi, and S. Turri, *Polymer*, **42**, 9723 (2001)
6. A. Wurtz, *Ann*., **71**, 326 (1849)
7. A. Gautier, *Ann*., **149**, 313 (1869)
8. A. Hofmann, *Ann*., **74**, 9 (1850)
9. W. Hentschel, *Ber*., **17**, 1284 (1884)
10. O. Bayer, *Angew. Chem*., **A59**, 275 (1947)
11. P. Schlack, *Ger. Pat. Appl*., *J-66330*, (1940)
12. A. Farkas, G. A. Mills, W. E. Emer, and J. B. Maerker, *Ind. Eng. Chem*., **51**, 1299 (1959)
13. R. E. Wittendorfer, *Anal*. *Chem*., **36**, 930 (1964)
14. P. C. Colodny, and A. V. Tobolsky, *J. Am. Chem. Soc*., **79**, 4320 (1957)
15. E. E. Gruber, and O. C. Keplinger, *Ind*. *Eng*. *Chem*., **51**, 151 (1959)
16. S. R. Sandler, and F. R. Berg, *J. Appl. Polym. Sci*., **9**, 3909 (1965)
17. C. B. Reilly, and M. Orchin, *Ind*. *Eng*. *Chem*., **79**, 4320 (1957)
18. S. N. lasbrenner, B. Golding, and L. C. Case, *Ind*. *Eng*. *Chem*., **51**, 1382 (1959)

19. W. Chang, R. L. Scriven, J. R. Peffer, and S. Proter, Jr., *Ind. Eng. Chem.* Prod. Res. Develop., **12**, 278 (1973)

20. N. H. Frick, H. L. Gerhart, H. E. Gilbert, and E. E. Parker, *Ind. Eng. Chem.*, **61**, 60 (1969)

21. D. Dieterich, *Prog. Org. Coat.*, **9**, 281 (1981)

22. R. L. Tirpark, and P. H. Markusch, *J. Coat. Technol.*, **58**, 49 (1986)

23. B. K. Kim, T. K. Kim, and H. M. Jeong, *J. Appl. Polym. Sci.*, **53**, 371 (1994)

24. D. R. Karsa, and W. D. Davis, "*Waterborne Coatings and Additives*", Royal society of Chemistry: Cambridge, U.K. (1995)

25. P. Schlack, *DBP 920512* (1943)

26. J. E. Mallonee, *U. S. Patent 2968572* (1961)

27. D. Dietrich, W. Keberle, and H. Witt, *Angew. Chem.*, **82**, 53 (1970)

28. D. Dietrich, E. Müller, O. Bayer, and J. Peter, *DBP 1495693* (1962)

29. A. Rembaum, W. Baumgarten, and A. Eisenberg, *J. Polym. Sci.*, **B6**, 159 (1968)

30. K. Noll, *U. S. Patent 3905929* (1973)

31. D. Dietrich, and O. Bayer, *U. S. Patent 3479310* (1963)

32. S. L. Hsu, H. X. Xiao, H. H. Szmant and K. C. Frisch, *J. Appl. Polym. Sci.*, **29**, 2467 (1984)

33. H. A. Al-salah, K. C. Frisch, H. X. Xiao and J. A. Mclean Jr., *J. Polym. Sci., Part A: Polym. Chem.*, **25**, 2127 (1987)

34. D. C. Lee, R. A. Register, C. Z. Yang and S. L. Cooper, *Macromolecules*, **21**, 1005 (1988)

35. C. K. Kim, and B. K. Kim, *J. Appl. Polym. Sci.*, **43**, 2295 (1991)

36. S. A. Chen and J. S. Hsu, *Polymer*, **34**, 2769 (1993)

37. S. A. Chen and J. S. Hsu, *Polymer*, **34**, 2776 (1993)

38. H. Xiao, H. X. Xiao, K. C. Frisch and N. Malwitz, *J. Appl. Polym. Sci.*, **54**, 1643 (1994)

39. Y. M. Lee, J. C. Lee and B. K. Kim, *Polymer*, **35**, 1095 (1994)

40. B. K. Kim and J. C. Lee, *J. Polym. Sci., Part A: Polym. Chem.*, **34**, 1095 (1996)

41. B. K. Kim and J. C. Lee, *Polymer*, **37**, 469 (1996)

42. D. J. Hourston, G. Williams, R. Satguru, J. D. Padget and D. Pears, *J. Appl. Polym. Sci.*, **66**, 2035 (1997)

43. D. J. Hourston, G. D. Williams, R. Satguru, J. C. Padget and D. Pears, *J. Appl. Polym. Sci.*, **74**, 556 (1999)

44. S. Asaoka, T. Sakurai, M. Kitajima and H. Hanazawa, *J. Appl. Polym. Sci*., **73**, 741 (1999)

45. J. E. Yang, J. S. Kong, S. W. Park, D. J. Lee and H. D. Kim, *J. Appl. Polym. Sci.*, **86**, 2375 (2002)

46. Y. S. Kwak, S. W. Park and H. D. Kim, *Colloid Polym. Sci.*, **281**, 957 (2003)

47. S. A. Madbouly, J. U. Otaigbe, A. K. Nanda, and D. B. Wicks, *Macromolecules*, **38**, 4014 (2005)

48. T. Tawa, and S. Ito, *Polym. J*. **38**, 686 (2006)

49. A. K. Nanda, and D. A. Wicks, *Polymer*, **47**, 1805 (2006)

50. W. Keberle, and D. Dietrich, *DBP 1495847* (1964)

51. G. N. Chen, and K. N. Chen, *J. Appl. Polym. Sci.*, **63**, 1609 (1997)

52. Y. S. Kwak, S. W. Park, Y. H. Lee, and H. D. Kim, *J. Appl. Polym. Sci.*, **89**, 123 (2003)

53. Piotr Król, Bożena Król, Lech Subocz, and Pawel Andruszkiewicz, *Colloid Polym. Sci.*, **285**, 177 (2006)

54. K. Noble, *Prog. Org. Coat.*, **32**, 131 (1997)

55. M. Melchiors, M. Sonntag, C. Kobusch, and E. Jürgens, **40**, 99 (2000)

56. Z. W. Wicks, D. A. Wicks, and J. W. Rosthauser, *Prog. Org. Coat.*, **44**, 161 (2002)

57. R. B. Pandey, and M. W. Urban, *Langmuir*, **20**, 2970 (2004)

58. D. B. Otts, L. A. Cueva-Parra, R. B. Pandey, and M. W. Urban, *Langmuir*, **21**, 4034 (2005)

59. D. B. Otts, and M. W. Urban, *Polymer*, **46**, 2699 (2005)

60. D. B. Otts, K. J. Pereira, W. L. Jarret, and M. W. Urban, *Polymer,* **46**, 4776 (2005)

61. T. Tawa, and S. Ito, *Colloid Polym. Sci.*, **283**, 781 (2005)

62. C. Hepburn, "*Polyurethane Elastomers*", Elsevier Applied Science Press: New York, Chapter 9. (1992)

63. G. Oertel, "*Polyurethane Handbook*", Hanser Press: Munich, Chapter 8. (1994)

64. L. L. Harrell, Jr., *Macromolecules*, **2**, 607 (1969)

65. R. A. Assink, *Macromolecules*, **11**, 1233 (1978)

66. J. J. Dumais, L. W. Jelinski, L. M. Leung, I. Gancarz, A. Galambos, and J. T. Koberstein, *Macromolecules*, **18**, 116 (1985)

67. H. J. Tao, D. M. Rice, W. J. MacKnight, and S. L. Hau, *Macromolecules*, **28**, 4036 (1995)

68. S. Velankar, and L. Cooper, *Macromolecules*, **33**, 395 (2000)

69. S. Sakurai, Y. Okamoto, H. Sakaue, T. Nakamura, L. Banda and S. Nomura, *J. Polym. Sci., Part B: Polym. Phys.*, **38**, 1716 (2000)

70. G. Consolati, M. Levi M and S. Turri, *Polymer*, **42**, 9723 (2001)

71. H. Tan, M. Guo, R. Du, X. Xie, J. Li, Y. Zhong and Q. Fu, *Polymer*, **45**, 1647 (2004)

72. Y. Chen, and Y. L. Chen, *J. Appl. Polym. Sci.*, **46**, 435 (1992)

73. Y. S. Kwak, S. W. Park, and H. D. Kim, *Colloid Polym. Sci.*, **281**, 957 (2003)

74. M. Salame, *Polym. Eng. Sci.*, **26**, 1543 (1986)

75. M. Salame, *J. Plast. Film Sheeting*, **2**, 321 (1986)

76. E. P. Giannelis, *Adv. Mater.*, **8**, 29 (1996)

77. E. P. Giannelis, *Appl. Organomet. Chem.*, **12**, 675 (1998)

78. S. S. Ray, and M. Okamoto, *Prog. Polym. Scit.*, **28**, 1539 (2003)

79. K. Yano, A. Usuki, and A. Okada, *J. Appl. Polym. Sci.*, **35**, 2289 (1997)

80. L. E. Nielsen, *J. Macromol. Sci. (Chem.)*, **A1**, 929 (1967)

81. R. K. Bharadwaj, *Macromolecules*, **34**, 9189 (2001)

82. G. H. Fredrickson, and J.Bicerano, *J. Chem. Phys.,* **110**, 2181 (1999)

83. A. A. Gusev, and H. R. Lusti, *Adv. Mater.*, **13**, 1641 (2001)

84. S. S. Ray, K. Yamada, M. Okamoto, A. Ogami, and K. Ueda, *Chem. Mater.*, **15**, 1456 (2003)

85. S. S. Ray, K. Okamoto, and M. Okamoto, *Macromolecules,* **30**, 4097 (2003)

86. S. Takahashi, H. A. Goldberg, C. A. Feeney, D. P. Karim, M. Farrell, K. O'Leary, and D. D. Paul, *Polymer*, **47**, 3083 (2006)

87. R. Xu, E. Manias, and A. J. Snyder, *Macromolecules*, **34** , 337 (2001)

88. J. H. Chang, and Y. U. An, *J. Appl. Polym. Sci. Polym. Chem.*, **40**, 670 (2002)

89. M. Tortora, G. Gorrasi, V. Vittoria, G. Galli, S. Ritrovati, and E. Chiellini, *Polymer*, **43**, 6147 (2002)

90. M. A. Osman, V. Mittal, M. Morbidelli, and U. W. Suter, *Macromolecules*, **36**, 9851 (2003)

Part I

Chapter 2

Preparation and Reactions of Water-Dispersible Isocyanate in Aqueous Medium

2.1. Introduction

Polyurethane is a unique polymeric material with a wide range of physical and chemical properties and it has been used in various fields, such as foams, coatings, adhesives, and thermoplastic elastomers. [1-4] Especially in the coating industry, polyurethane occupies an established position in many applications, because the coating layer has a high quality, for example, resistance to solvents, weather stability and mechanical properties.

There are two major systems in polyurethane coatings. One is called a one-component (1K) system in which the substrate is coated with high molecular weight polyurethane and dried physically. The other is a two-component (2K) system which is a combination of hydroxyl functional polymers and polyisocyanate hardeners containing NCO group. In the past, maximum performance and appearance were the main requirements, resulting in the marked development of solventborne 2K systems. In recent years, however, the demand has shifted to reduce volatile organic compounds (VOCs) and hazadous air pollutants (HAPs) emission. The waterborne polyurethane system is one of the options for reducing VOCs and HAPs. [5-11]

Until the late 1980's, a waterborne 2K polyurethane (WB 2K-PU) system was unthinkable for two main reasons. Firstly, the isocyanate is usually hydrophobic and it is

difficult to disperse into the water. Secondly, there is an undesired side reaction between the NCO group and water as shown in Scheme 2-1. The former problem was solved by the development of a novel type of water-dispersible isocyanate (WDPI), which was modified with hydrophilic groups.[12, 13] For example, WDPI were produced by reacting monohydroxy-functional polyethylene glycols with some of the NCO groups of the polyisocyanate. NCO groups, however, are highly reactive and it is difficult to suppress the side reaction between NCO groups and water.[14-20]

In utilization of WB 2K-PU system, it is important to keep NCO groups in aqueous solution for a long time (to achieve long pot-life) by suppressing the side reaction between NCO and water. To attain these contradictory purposes, the new WDPI, which was the hexamethylene diisocyanate (HDI) allophanate modified with methoxy polyethylene glycols (MPEG), was prepared in this research. The reactivity of the NCO group in terms of the residual NCO group content in water, particle size, pH, molecular weight and mechanical properties were investigated by using this WDPI. This new WDPI could be dispersed into water in a simple way because of the very low viscosity. A long lifetime of NCO units could be attained by adjusting the MPEG content. In addition, the internal structure of the WDPI micelles in relation to the NCO reactivity is discussed.

Scheme 2-1. Reactions of isocyanate with hydroxyl group and water.

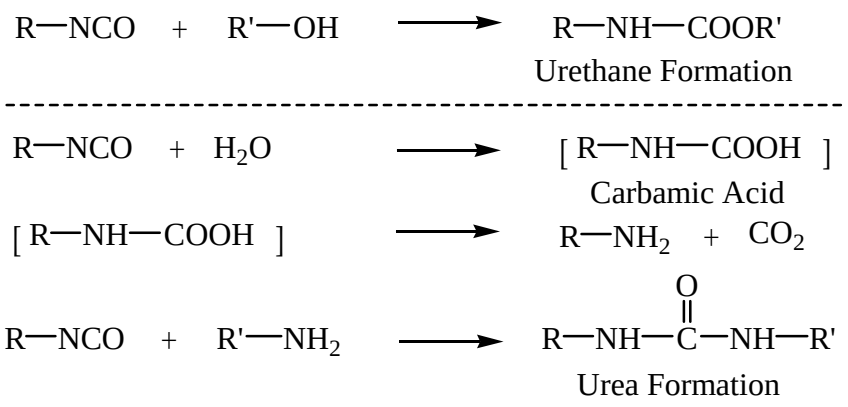

2.2. Experimental

2.2.1. Materials

Hexamethylene diisocyanate (HDI, Wako Pure Chemical Industries, Ltd.), 2-methyl-1-propanol (Wako Pure Chemical Industries, Ltd.), tris(tridecyl)phosphite (Johoku Chemical Co. Ltd.), lead 2-ethyl-hexanicacid (Wako Pure Chemical Industries, Ltd.), benzoyl chloride (Wako Pure Chemical Industries, Ltd.) were used without further purification. Methoxy polyethylene glycol (MPEG, NOF Corp.) was dried at 70 ˚C for 5 h under nitrogen bubbling.

The polyurethane dispersion (PUD) for mechanical test was separately prepared with polytetramethylene oxide glycol (PTMG: Mn = 2,000), triethylene glycol, dimethylol propionic acid (DMPA), 1,3-bis(isocyanatemethyl)cyclohexane, triehylamine and 2-(2-aminoethylamino)ethanol. This product contains 5,000 COOH group and 3,800 OH group equivalent.

2.2.2. Sample Preparation

WDPIs were synthesized in four steps as shown in Scheme 2-2. The first step is the urethane reaction between HDI and 2-methyl-1-propanol. HDI (5.77 mol), 2-methyl-1-propanol (0.405 mol) and tris(tridecyl) phosphite (0.795 mmol) were mixed at 20 ˚C under nitrogen atmosphere and heated at 80 ˚C for 2 h. This reaction was performed under excess amounts of NCO in order to leave one of two NCO groups in HDI after the reaction with an OH group of 2-methyl-1-propanol.

The second step is the allophanate reaction. To the solution was added lead 2-ethylhexanic acid (1.01 mmol) as a catalyst kept at 90 ˚C for 1 h, and then benzoyl chloride (0.711 mmol) was added as a termination agent.

Scheme 2-2. Preparation process for WDPI.

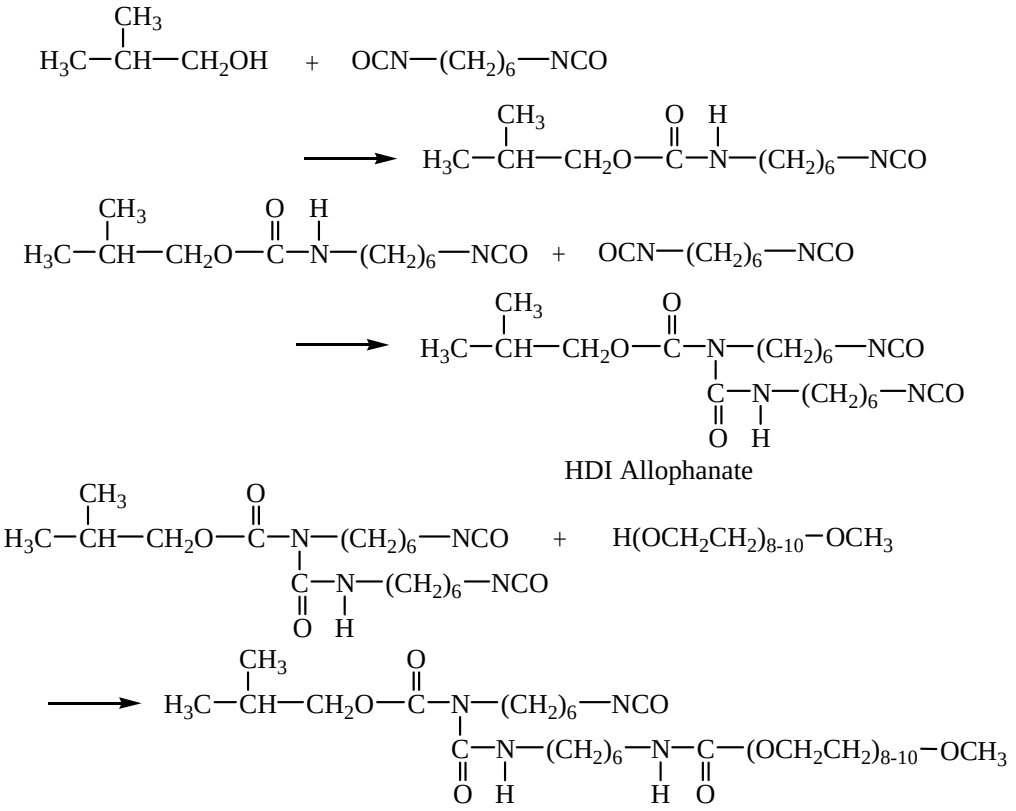

The third step is distillation to remove unreacted HDI by using the thin membrane distillation method at 140 ˚C and 0.5 mmHg. [21]

In the final step, part of the NCO group of HDI allophanate reacted with the OH group of MPEG 4 h at 70 ˚C. Four WDPIs with different contents and molecular weights of MPEG were prepared as shown in Table 2-1. Samples were designated so that, for example in A400(20), the initial letter 'A' refers to allophanate, 400 to the molecular weight of MPEG, and 20 to the MPEG weight ratio (%) in this WDPI. This final reaction proceeded under excess amounts of NCO group compared to OH group of MPEG so that the samples are a two-compound mixture; one is HDI allophanate modified with MPEG and the other is without MPEG as shown in Scheme 2-2. The content of HDI allophanate modified with MPEG was evaluated by NCO equivalent

Table 2-1. Characteristics of WDPIs.

Sample	A400(15)	A400(20)	A400(25)	A550(20)
MPEG M_n	400	400	400	550
MPEG content (wt %)	15	20	25	20
MPEG content (mmol/g)	3.14	4.18	5.23	4.18
NCO content (mmol/g)	3.41	3.05	2.65	3.18
HDI allophanate with MPEG (mol %)	21.0	29.9	42.4	22.6
Viscosity (mPa·s at 25 ºC)	184	230	274	240

measurement and the results are shown in Table 2-1.

2.2.3. Dispersion Preparation

To investigate the lifetime of NCO groups in water, the aqueous dispersion samples were prepared by addition of WDPI into water with stirring, yielding stable dispersion of a 30 wt % concentration. The dispersion was left standing at 25 ºC and a part of it was examined every 1 h after dispersing.

2.2.4. Sample Preparation for Mechanical Test

To study the influence of the NCO lifetime in water on the mechanical properties of a WB 2K-PU system, A400(20) was dispersed into water and kept for 10 min, 4 h and 5 h, and then it was mixed with PUD. The ratio with NCO of A400(20) and OH of PUD is 1.2. Film samples for mechanical measurements were prepared by casting the mixed dispersions on a metal plate under ambient conditions. The films (about 0.1 mm thickness) were dried for more than 1 day and kept at 130 ºC for 1 h to remove the remaining moisture.

2.2.5. Measurements

NCO content was measured by the dibutylamine back-titration method as follows.

The dispersion sample containing a NCO group was dissolved in THF. Dibutylamine was added to the THF solution with stirring and the amine group reacted with the NCO group immediately. This solution was diluted with isopropanol and the residual amine group of dibutylamine was titrated by 0.1 N HCl aq..

The average particle size was measured by light scattering (Coulter N4 Plus), where a He-Ne laser with wavelength of 632.8 nm was used. The sample was diluted in diionaized water to adequate concentration for measurement.

Infrared spectroscopic experiments were performed with a fourier transform infrared spectrometer (HORIBA FT-710). The samples for IR measurements were diluted in THF to a 1 % solution and coated on a NaCl disk. In order to remove the residual water and THF solvent, the disk was placed under a nitrogen stream at 25 ºC for 10 min.

The pH values were measured with a HORIBA M-13 pH meter. A part of this WDPI dispersion was extracted and used for pH measurement.

The samples for GPC measurement were prepared by addition of each dispersion sample to methanol and heated at 50 ºC for 24 h. Active NCO groups of the WDPI terminated with OH groups of methanol and residual methanol and water were removed by evaporation. The molecular weights of these samples were determined with a Waters 410 system with DMF. The calibration curves for GPC were obtained by using polystyrene standard samples.

Mechanical properties were measured at room temperature using INTESCO Model 205 following the ASTM D412 specifications. A crosshead speed of 300 mm/min was used throughout these investigations to determine the ultimate tensile strength and elongation at break for all the samples. The values quoted are the average of five measurements.

2.3. Results and Discussion

2.3.1. Lifetime of NCO Group in Water: MPEG Content Dependence

Three samples, A400(15), A400(20) and A400(25) (Table 2-1), in which the MPEG parts have the same molecular weight of 400 and 15, 20 and 25 % weight fractions of MPEG, were selected respectively. Figure 2-1 shows the residual NCO contents in water with the elapse of time after dispersing WDPI into water. Here, the residual NCO content just after dispersing is regarded as 100 %.

As Figure 2-1 shows, the reactivity is quite different among three samples. For A400(15), the residual NCO content was about 70 % even at 7 h after dispersing. On the other hand, that of A400(20) markedly decreased after 4 h and was found to be less than 10 % at 5 h. In the case of A400(25), it started decreasing at 2 h and was almost nothing after 3.5 h. These results show that the reduction of NCO groups in water has an

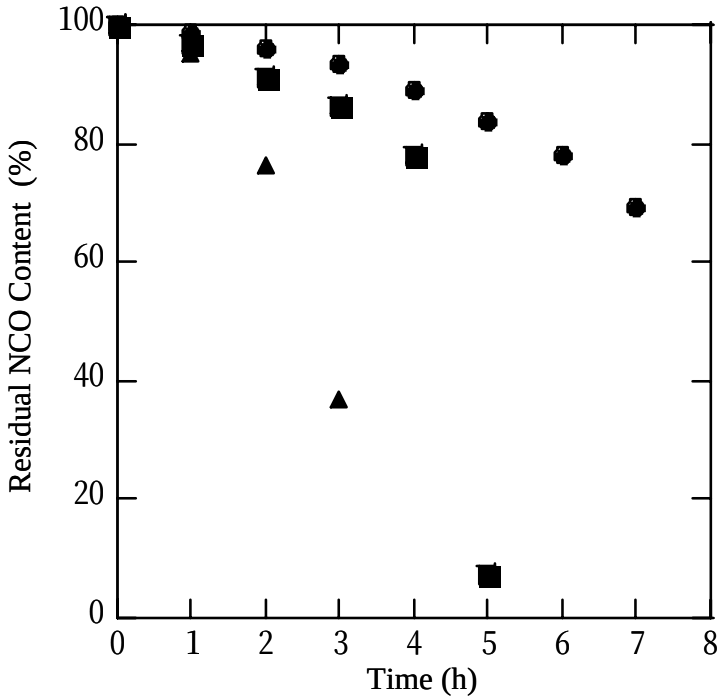

Figure 2-1. Residual NCO contents of WDPI in water at various contents of MPEG: *filled circle* (●) A400(15), *filled square* (■) A400(20), *filled triangle* (▲) A400(25).

induction period and it is accelerated as the content of hydrophilic group increases.

Next, the average particle diameters of WDPI dispersions were measured. Figure 2-2 shows the particle diameter after dispersion and the initial value is 265 nm for A400(15), 195 nm for A400(20), and 171 nm for A400(25). The higher the content of MPEG is, the smaller the particle diameter is, due to the hydrophilic character of MPEG. As shown in Figures 2-1 and 2-2, it is obvious that the smaller the particle diameter of this dispersion is, the faster the reduction of NCO groups is, because the NCO groups in the smaller particle are easily attacked by water molecules and react with water. Furthermore, the particle diameter is found to change markedly at 5 h for A400(20) and at 3.5 h for A400(25). The rapid reduction of NCO groups in water has some influence on the particle diameter. It is worth noting that the bubbling of the solution was observed simultaneously with the rapid decrease of NCO content.

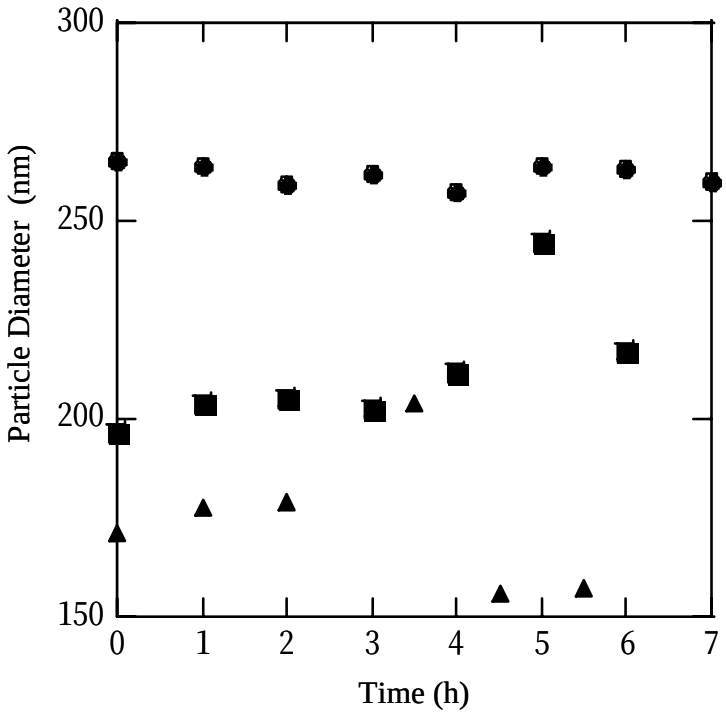

Figure 2-2. Particle diameters of WDPI dispersions at various contents of MPEG: *filled circle* (●) A400(15), *filled square* (■) A400(20), *filled triangle* (▲) A400(25).

2.3.2. Lifetime of NCO Group in Water: MPEG Molecular Weight

The relationship between MPEG molecular weight and the lifetime of NCO group in water was examined using A400(20) and A550(20). These two samples have the same content of MPEG unit, but a different molecular weight, in other words, a different chain length. Figure 2-3 shows the residual NCO contents of them as a function of time after dispersing at 25 ºC, where the residual NCO content just after dispersing WDPI into water is regarded as 100%. The reactivity of NCOs in these samples was similar throughout the observation period. In both A400(20) and A550(20), the residual NCO contents were more than 70 % at 4 h and remarkably decreased within the next 1 h. These results indicate that the reduction of NCO groups in water is independent of the chain length of polyoxyethylene. The average diameters of both dispersions are almost

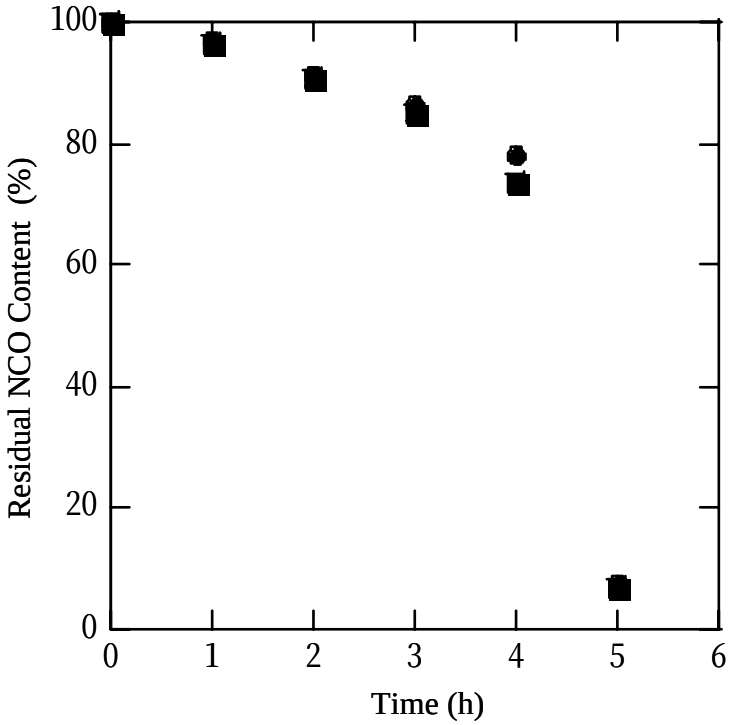

Figure 2-3. Residual NCO contents of WDPI in water at different molecular weight of MPEG: *filled circle* (●) A400(20), *filled square* (■) A550(20).

the same value of about 200 nm, suggesting that the lifetime is largely dependent on the diameter of the dispersion and the diameter is not determined by molecular weight, but by the content of MPEG in this WDPI.

2.3.3. Reaction of WDPI in Water

The reaction between NCO group and water was followed by FTIR spectroscopy. A400(20) was selected as the sample for FTIR measurement. Examples of FTIR spectra collected at different times after dispersion are presented in Figure 2-4: 10 min, 2 h, 4 h,

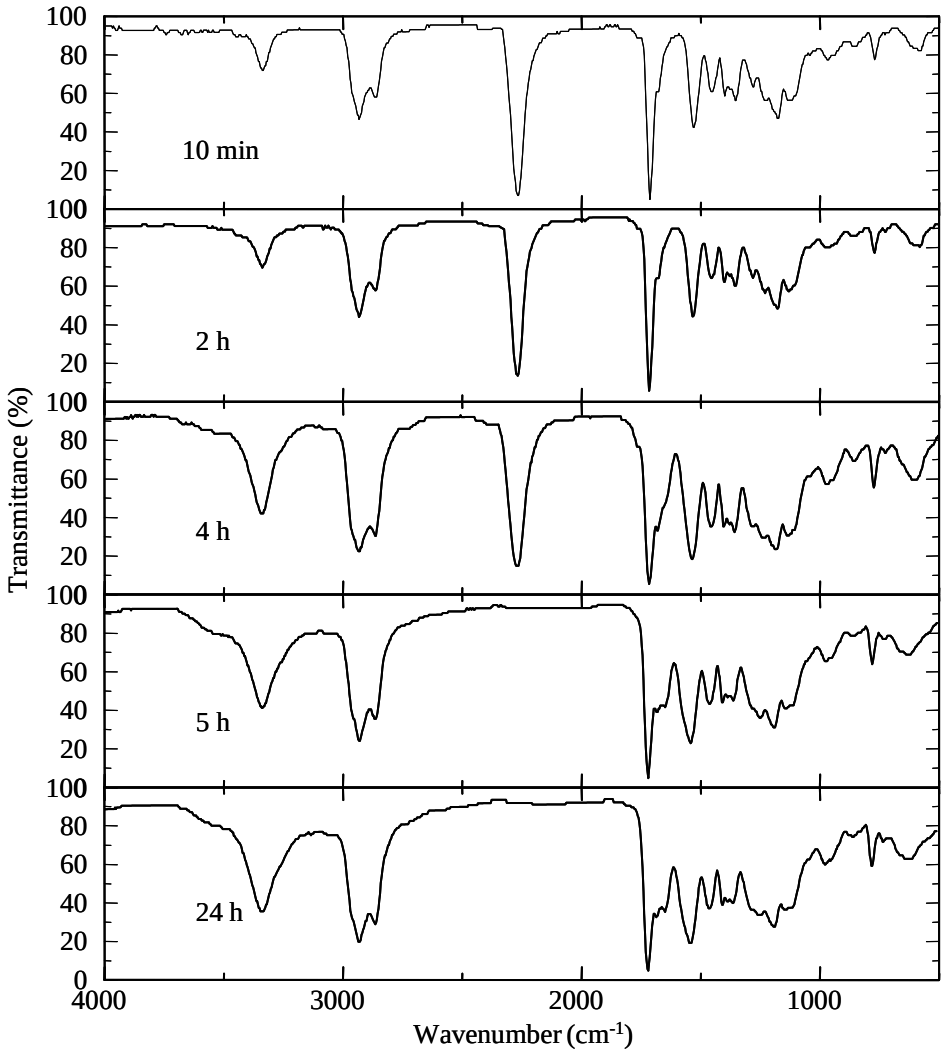

Figure 2-4. FT-IR spectra of A400(20): the spectra at 10 min, 2, 4, 5, and 24 h after dispersing A400(20) into water from top to bottom.

5 h, and 24 h from the top to bottom, respectively. The 2,270 cm^{-1} peak in the FTIR spectra is assigned to NCO groups of WDPI. As shown in Figure 2-4, this 2,270 cm^{-1} peak is clearly perceived at 10 min, 2 h and 4 h, but suddenly disappeared at 5 h. These results agree with the rapid decrease of NCO content as shown in Figure 2-1. By contrast, the 3,340 cm^{-1} peak and the 1,645 cm^{-1} peak, which are assigned to the urea group formed by the reaction between NCO and water, gradually increased with the passage of the time.

The pH values of A400(20) dispersion were also monitored as shown in Figure 2-5. The pH values are stable around 6.0 until 3 h and then gradually increase between 3 h and 5 h. These results also indicate that the rapid reaction between the NCO group and water gives influence on pH of this aqueous dispersion.

This reaction process between NCO and water was examined by the GPC

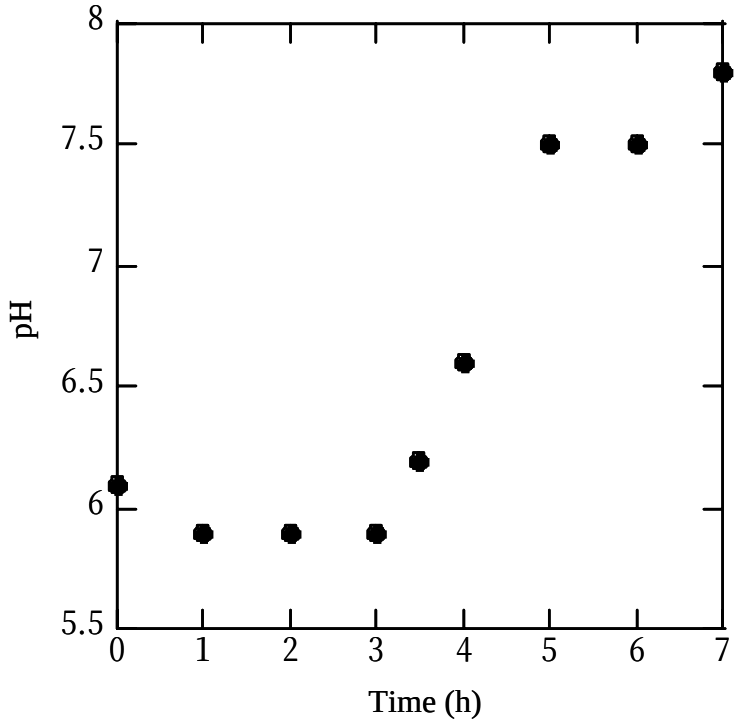

Figure 2-5. pH values of A400(20) aqueous dispersion during the time after dispersing A400(20) into water.

measurement in more detail. Figure 2-6 shows the GPC chromatograms at 10 min, 2 h, 4 h, 5 h, and 24 h after dispersing A400(20) into water. There are two main peaks at 10 min, of which one peak at the elution time of 35 min is assigned to the HDI allophanate without MPEG, and the other peak at 34 min is due to HDI allophanate modified with MPEG. With the elapse of time, the GPC chromatograms are slightly changed until 4 h.

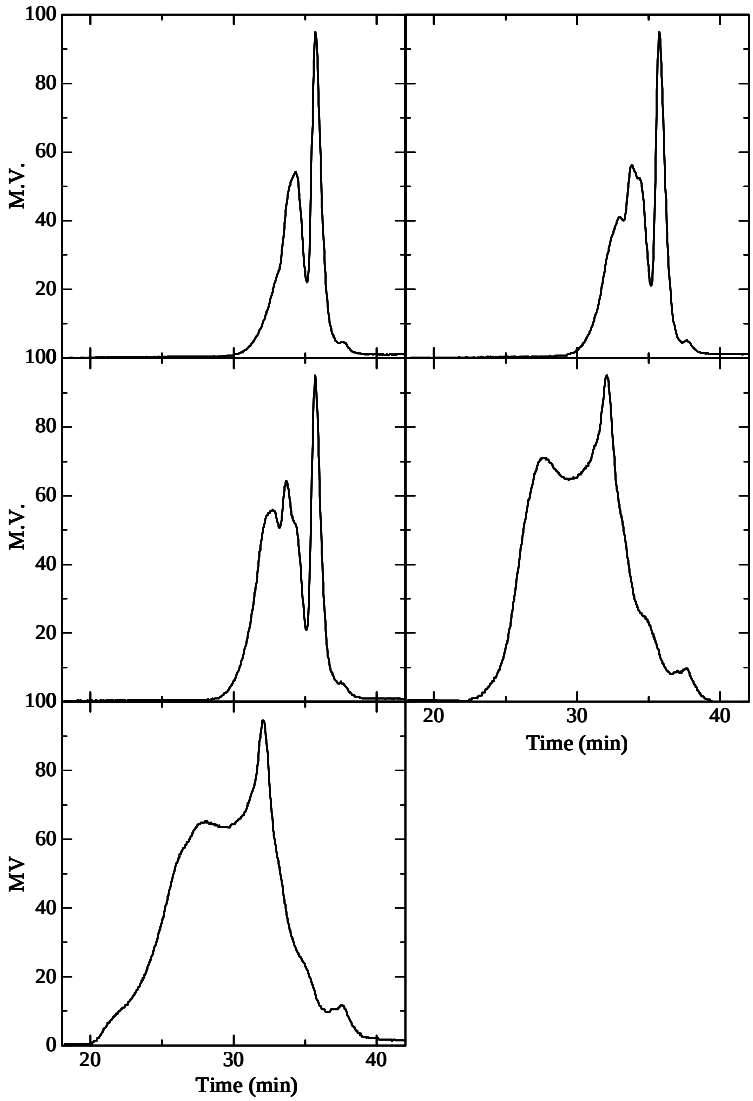

Figure 2-6. The GPC chromatogram of A400(20): the chromatogram are at 10 min (*top left*), 2 h *(top right*), 4 h (*middle left*), 5 h (*middle right*) and 24 h (*bottom left*) after dispersing A400(20) into water.

The new peaks at 32 and 33 min on the chromatogram appear with the decrease of the peaks at 34 and 35 min, while the peak at 35 min remains until 4 h. This GPC chromatogram changes drastically at 5 h. The peak at 35 min disappears completely and a broad peak, which means the production of much higher molecular weight molecules, appears at the shorter elution time. At 24 h, the broad peak is shifted to a shorter elution time compared to that at 5 h. These results of GPC measurements show that a large amount of A400(20) NCO groups reacts with water in the time range between 4 and 5 h and yields a high molecular weight compound.

This sudden reaction between NCO and water is probably caused by the core-shell structure of this WDPI micelle, as shown in Figure 2-7. This WDPI consists of two components, one is HDI allophanate without MPEG and the other is HDI allophanate with MPEG. HDI allophanate without MPEG exists near the center of this dispersion and forms the core of micelles. By contrast, HDI allophanate modified with MPEG exists near the surface of this dispersion and forms the shell. The reaction proceeds preferentially in the shell at the early stage, because the hydrophobic core region is protected from the penetration of water.

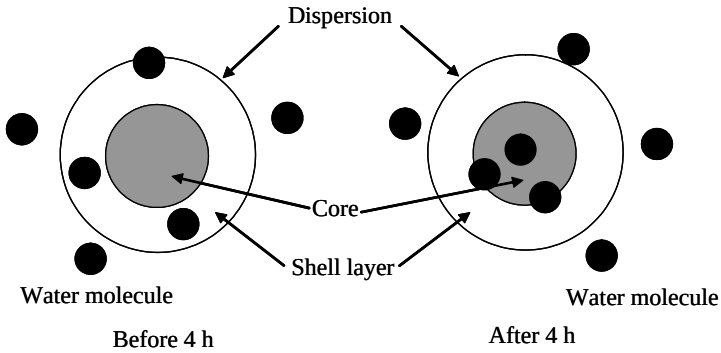

Figure 2-7. The illustration of hydrophilic isocyanate dispersion structure: water molecule attacks only shell layer before 4 h (*left*), and water molecule attacks the core after 4 h (*right*).

Taking into account these two components, three kinds of NCO reactions can be considered as shown in Scheme 2-3. A is a coupling reaction of two HDI allophanates bearing the MPEG unit, B is an extension reaction between HDI allophanates with MPEG and without MPEG, and C is a polymerization reaction of bifunctional HDI allophanates without MPEG. Because the HDI allophanate modified with MPEG exists near the surface of dispersion and easily comes in contact with water, reaction A mainly takes place and forms dimeric compounds in the early stage of reaction until 4 h. Reaction B also proceeds until 4 h, yielding the peak at 32 min on the chromatogram as the product. Until 4 h, almost all NCO groups existing in the shell layer has been consumed and HDI allophanates without MPEG start reacting with water. At this time point, the type of reaction changes to C, because water molecules reach the interface of the core region of this dispersion. Therefore most HDI allophanates without MPEG rapidly react with water and form much higher molecular weight compounds after 4 h as shown in Figure 2-6. The rapid change between 4 and 5 h is probably due to the

Scheme 2-3. Three kinds of reactions between NCO group and water.

(A) Coupling reaction of two HDI allophanates with MPEG

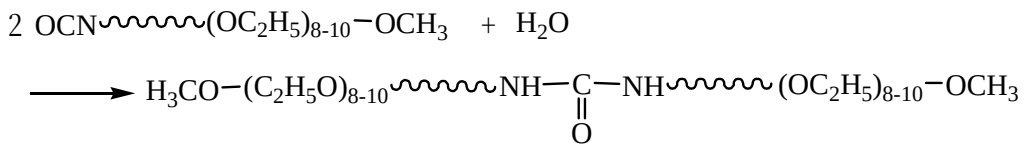

(B) Extension reaction between HDI allophanate with MPEG and without MPEG

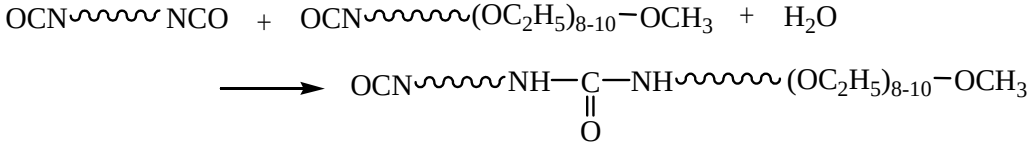

(C) Coupling and polymeric reaction between two HDI allophanate without MPEG

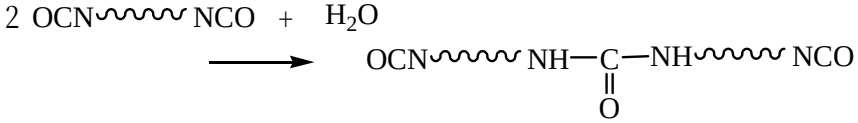

difference in NCO concentration of two layers. The NCO concentration is low in the shell layer, because HDI allophanate modified with MPEG is the main component of the shell. Therefore, the reaction between NCO and water proceeds slowly. On the other hand, the NCO concentration is high in the core, which is composed of HDI allophanates without MPEG. Consequently, the reaction between NCO and water proceeds very quickly.

2.3.4. Mechanical Properties of Film Formed by WDPI and Polyurethane Dispersion

The influence of the NCO lifetime in water on the mechanical properties of a two-component (2K) polyurethane system was studied. Table 2-2 shows the tensile strengths and ultimate elongation for each sample. Reference is the mechanical property of the film formed by polyurethane dispersion without A400(20). The ultimate elongation was decreased and the tensile strengths of 500 % and 700 % elongation were increased by adding A400(20). This result indicates that NCO group of A400(20) reacted with OH group of polyurethane dispersion and formed crosslinking structure. Furthermore, there is no big difference between the ultimate elongation of 10 min and 4 h samples. This indicates that almost all NCO group of A400(20) is maintained for 4 h

Table 2-2. Mechanical properties of 2K polyurethane system.

Sample	10min	4h	Ref.
100% Strength (N/mm^2)	1.33	1.39	1.33
300% Strength (N/mm^2)	1.94	1.91	1.90
500% Strength (N/mm^2)	3.10	3.18	2.99
700% Strength (N/mm^2)	14.4	13.8	12.4
Tensile strength (N/mm^2)	28.0	30.2	41.3
Elongation (%)	784	812	901

in water. The A400(20) dispersion passed 5 h were tried to mix to polyurethane dispersion, but two dispersions could not be mixed, and formed inhomogeneous film not suitable for measurement. This is due to the sudden reaction between NCO and water. After 5 h, the rapid progress of NCO reaction yields high molecular weight, which is not mixed with polyurethane dispersion any longer.

2.4. Conclusion

A novel WDPI was synthesized by the reaction of HDI allophanate with MPEG. This WDPI had a very low viscosity and formed stable dispersion with a simple mixing method into water. The NCO lifetime in water was closely related to the particle diameter of this dispersion, and the diameter was not determined by molecular weight but by the content of MPEG in this WDPI. As the MPEG content increased, the diameters of this dispersion became small, resulting in the short NCO lifetime in water. The results of FTIR and GPC measurements suggested that the types of reactions between the NCO and water molecules changed stepwise with the elapse of time, depending on the location of the reaction inside the micelles. The rapid consumption of NCO groups after a long induction period could be interpreted by the core-shell structure of micelles, in which the shell layer mainly consisted of HDI allophanate modified with MPEG and the core was composed of hydrophobic diisocyanates without MPEG. These results clearly indicate that NCO lifetime of WDPI in water is adjustable by designing the micellar structure on the balance of hydrophobic HDI and hydrophilic MPEG components.

References

1. M. F. Sonnenschein, N. Rondan, B. L. Wendt, and J. M. Cox, *J. Polym. Sci. Part A: Polym. Chem*., **42**, 271 (2004)
2. W. Tang, R. J. Farries, W. J. Macknight, and C. D. Eisenbach, *Macromolecules*, **27**, 2814 (1994)
3. T. K. Chen, Y. I. Tien, and K. H. Wei, *Polymer*, **41**, 1345 (2000)
4. G. Consolati, M. Levi, and S. Turri, *Polymer*, **42**, 9723 (2001)
5. D. Dieterich, *Prog. Org. Coat*., **9**, 281 (1981)
6. J. W. Rosthauser, and K. Nachtkamp, *J. Coat. Fabrics*, **16**, 39 (1986)
7. B. K. Kim, and J. C. Lee, *Polymer*, **37**, 469 (1996)
8. B. Vogt-Birnbridh, *Prog. Org. Coat*., **29**, 31 (1996)
9. Y. Mori, M. Yamazaki, .ans H. Shido H, *Prog. Org. Coat*., **40**, 119 (2000)
10. Y. B. Kim, H. K. Kim, J. K. Yoo, and J. W. Hong, *Surf. Coat. Tech*., **157**, 40 (2002)
11. J. E. Yang, J. S. Kong, S W. Park, D. J. Lee, and H. D. Kim, *J. Appl. Polym. Sci*., **86**, 2375 (2002)
12. P. B. Jacobs, and P. C. Yu, *J. Coat. Tech*., **65**, 822, 45 (1993)
13. C. R. Hrgedus, A. G. Gilicinski, and R. J. Haney, *J. Coat. Tech*., **68**, 852, 51 (1996)
14. M. J. Dorchak, *J. Coat. Tech*., **69**, 866, 47 (1997)
15. M. Melchiors, M. Sonntag, C. Kobusch, and E. Jurgens, *Prog. Org. Coat*., **40**, 99 (2000)
16. Z. W. Wicks Jr., D. A. Wicks, and J. W. Rosthauser, *Prog. Org. Coat*., **44**, 161 (2002)
17. W. Collong, A. Gobel, B. Kleuser, W. Lenhard, and M. Sonntag, *Prog. Org. Coat*., **45**, 205 (2002)

18. M. Bock, and J. Petzoldt, *Mod. Paint Coat*., **86**, 22 (1996)

19. Z. A. He, W. J. Blank, and M. E. Picci, *J. Coat. Tec*., **74**, 930, 31 (2002)

20. S. X. Feng, P. Lunney, and R. Wargo, *J. Coat. Tec*., **71**, 897, 143 (1999)

21. T. Nakashima, H. Shimizu, and F. Hirata, Jpn. Kokai. Tokkyo Koho JP H09-188566

Chapter 3

Microviscosity of the Reactive Water-Dispersible Polyisocyanate Micelle as Studied by Fluorescence Probe Techniques

3.1. Introduction

In the previous Chapter, a new WDPI was prepared, which forms the stable micelle in the aqueous medium.In waterborne 2K system, the influence of water is far important as compared with solventborne one, because a lot of water molecules are around the WDPI micelle and react with isocyanate groups of the WDPI. Therefore, the examination on the change of the WDPI micelle in aqueous medium with the reaction between NCO groups and water is significant. Microviscosity is as a measure reflecting the environment of micelle. The effective method to examine the microviscosity in the micelle is the fluorescence technique, because the fluorescence emission sensitively probes the environment in the vicinity of the fluorescent molecule. The rate of excimer formation is one index reflecting the microviscosity of the micelle because the excimer formation is a bimolecular and diffusion-controlled process between two molecules in the excited and ground states. [1-9] The fluorescence depolarization gives useful information for the microviscosity of the micelle. The fluorescence depolarization process is based on the rotational motion of the excited molecule during its fluorescence lifetime, so that fluorescence anisotropy reflects the microviscosity around the fluorescence molecule. [10-16]

Using the new WDPI, the microviscosity of the aqueous WDPI micelle was

evaluated by two fluorescence methods probing the translational and rotational diffusivities through the rate of excimer formation and the fluorescence depolarization, respectively. In this chapter, the interior microviscosity of the WDPI micelle is discussed by analyzing the fluorescent behavior.

3.2. Experimental

3.2.1. Materials

The details on the synthesis of the WDPI were described in Chapter 2. Figure 3-1 shows the chemical structures of components, which are hexamethylene diisocyanate allophanate (HDIA) and HDIA reacted with MPEG (HDIA-MPEG). The molar ratio of HDIA to HDIA-MPEG was 7 : 3, and the viscosity of WDPI was 0.23 Pa · s.

Pyrene and perylene (Wako Pure Chemical Industries, Ltd) were used as purchased. The fluorescent dye was dissolved in WDPI with concentrations from $1.0 \cdot 10^{-2}$ to $2.0 \cdot 10^{-1}$ M for pyrene and $6.0 \cdot 10^{-3}$ M for perylene. The WDPI was poured into water (30 wt%) with stirring, yielding the stable aqueous micelle dispersion. The diameter of the WDPI micelle is ca. 200 nm, which was measured by the dynamic light scattering method.

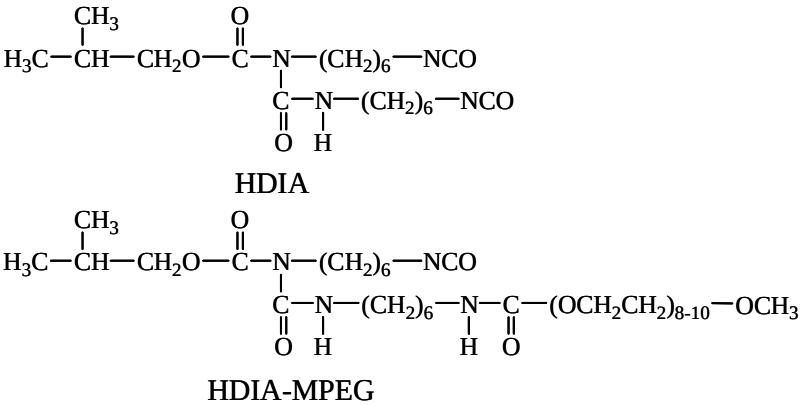

Figure 3-1. The structure of water-dispersible polyisocyanate (WDPI).

In order to estimate the microvisocosity by fluorescence depolarization, three other WDPIs with different viscosities were prepared by using HDI isocyanurates with different molecular weights instead of HDIA. The viscosities of WDPIs are 0.42, 0.80, and 1.8 Pa · s, respectively.

3.2.2. Measurements

Steady-state fluorescence measurements were curried out by a spectrometer (F-4500, HITACHI). Pyrene was used as the fluorescence probe in the measurement of the excimer formation rate. The micelle solution of the WDPI with pyrene was kept at a constant temperature of 25 ˚C. It was sampled every one hour after dispersing and then it was diluted by 2500 times with water for the fluorescence measurement. The fluorescence decay was measured by the time-correlated single photon counting method. The excitation light source was the third harmonic (295 nm) of a mode-locked Ti:sapphire laser (Tsunami, Spectra-Physics) pumped by an Ar^+ laser (BeamLok 2060, Spectra-Physics). The fluorescence emission was detected by a photomultiplier tube (R3234, Hamamatsu Photonics) through a monochoromator (MC-10N, Ritsu) with a long-pass filter (UV-37, Hoya) to cut the excitation light. The full width at halt maximum of the instrument response function (IRF) was 500 ps. The decay data were fitted to a multi-component exponential function convoluted with the IRF by the nonlinear least-square method.

In the fluorescence depolarization measurement, perylene was used as the fluorescence probe. Perylene is a suitable probe to examine the microviscosity inside the micelle because of the high limiting degree of depolarization, [10] the high fluorescence quantum yield and the short fluorescence lifetime (ca. 5 ns). [17, 18] The micelle solution was diluted by 1000 times with water for the fluorescence

depolarization measurement. The steady-state fluorescence anisotropy was measured by the spectrometer equipped with polarizers. Perylene was excited at 400 nm and the emission was measured at 473 nm. The steady-state fluorescence anisotropies were measured at 25 ˚C.

3.3. Results and Discussion

3.3.1. Location of Fluorescence Molecules

The fluorescence spectrum of WDPI / pyrene at an extremely low pyrene concentration of $2.4 \cdot 10^{-5}$ M in the aqueous micelle solution is shown as the solid curve in Figure 3-2. The spectrum has a structureless emission band at the longer wavelength (> 440 nm) due to the pyrene excimer in addition to the characteristic structured band of the monomer emission at 370 - 420 nm. On the other hand, the WDPI solution in ethyl acetate was also prepared under the same condition as the aqueous WDPI micelle; the WDPI / pyrene mixture at a pyrene concentration of $2.0 \cdot 10^{-1}$ M was added to the 2500

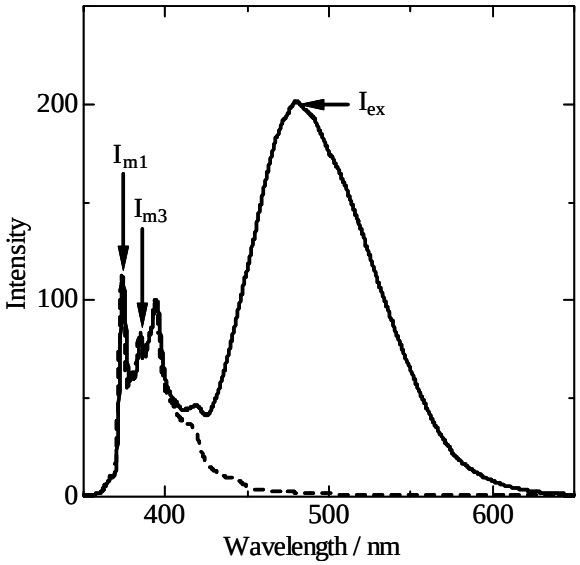

Figure 3-2. Fluorescence spectra of the aqueous micelle solution (solid line) and ethyl acetate solution (broken line). Pyrene concentration is $2.4 \cdot 10^{-5}$ M.

times amount of ethyl acetate, resulting in the pyrene concentration of $2.4 \cdot 10^{-5}$ M. The fluorescence spectrum for the ethyl acetate solution is also shown in Figure 3-2 as the broken line, indicating no excimer emission. In the ethyl acetate solution, the pyrene molecules uniformly exist because of the high solubility of pyrene in ethyl acetate. On the other hand, the pyrene molecules in the aqueous dispersion system of the WDPI cannot distribute homogeneously due to the low solubility to water (saturated concentration: $6.0 \cdot 10^{-6}$ M); therefore, pyrene is concentrated in the WDPI micelle. Assuming that the volume of WDPI is equal to that of the micelle, the apparent concentration of pyrene in the micelle $[Py]_{app}$ is estimated to be $2.0 \cdot 10^{-1}$ M. Such the high $[Py]_{app}$ resulted in the excimer emission.

The microscopic environment of pyrene is further discussed. The WDPI micelle forms the core-shell structure consisting of the hydrophilic HDI-A-M and the hydrophobic HDIA. The intensity ratio between the third (386 nm) and the first (375 nm) monomer emission peaks (I_{m3} / I_{m1}) of the pyrene spectrum depends on the environmental polarity of the dissolved pyrene molecules. [19-21] Therefore, the microscopic environment surrounding the pyrene molecule can be estimated from the value of I_{m3} / I_{m1}. Table 3-1 shows the value of I_{m3} / I_{m1} measured from the emission spectrum of pyrene in water, MPEG, HDI and the aqueous WDPI micelle. The pyrene

Table 3-1. The I_{m3}/I_{m1} value of pyrene emission spectra in water, MPEG, HDI, and the aqueous WDPI micelle. The pyrene concentration is $1.2 \cdot 10^{-5}$ M in each medium.

	I_{m3}/I_{m1}
Water	0.679
MPEG400	0.645
HDI	0.795
WDPI Micelle	0.787

concentration was $1.2 \cdot 10^{-5}$ M in each medium. The I_{m3} / I_{m1} value of the aqueous WDPI micelle (0.787) is closer to that of HDI (0.795) than MPEG (0.645). Accordingly, the pyrene molecules were in the more hydrophobic environment, that is, they mainly existed in the core of the micelle.

3.3.2. Microviscosity of WDPI Micelle Estimated by Excimer Formation Rate of Pyrene

As shown in the photophysical processes indicated in Figure 3-3, the excimer formation is a bimolecular process between the molecules in the ground and excited states. The excimer formation is diffusion-controlled; [22, 23] therefore, the rate of formation gives the information on the viscosity of the micelle core. Figure 3-4 shows the time evolution of the fluorescence spectra of pyrene in the aqueous WDPI micelle at $[Py]_{app} = 2.0 \cdot 10^{-1}$ M. The fluorescence spectrum drastically changed at 4.8 h and the ratio of the intensity of excimer emission to that of the monomer emission (I_{ex} / I_{m1})

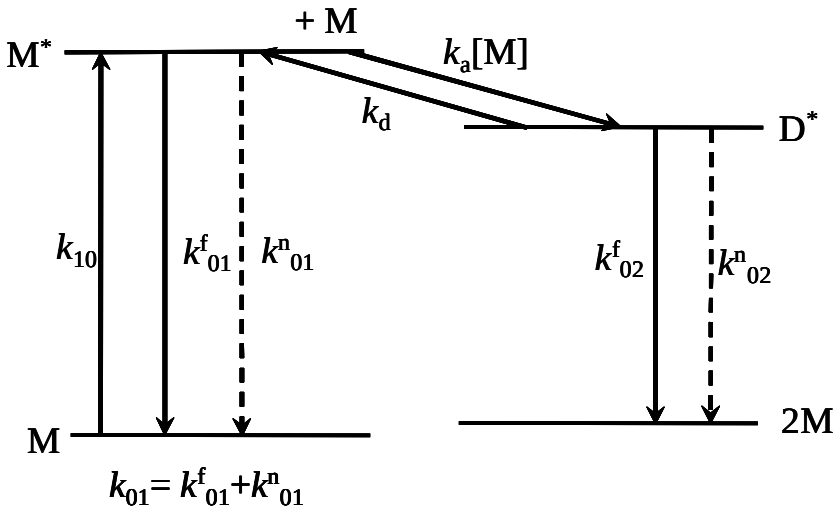

Figure 3-3. Rate processes in monomer and excimer system. The solid and broken lines indicate radiative and radiationless processes, respectively.

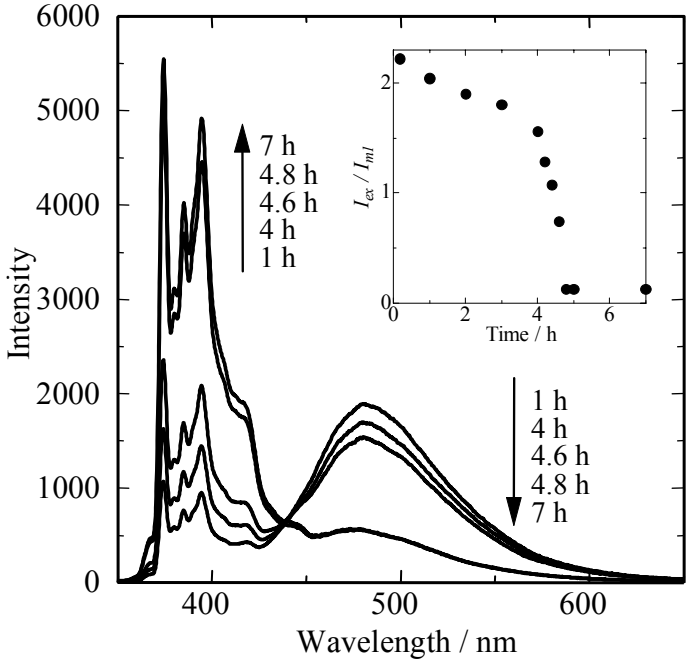

Figure 3-4. Fluorescece spectra after dispersing into water at $[Py]_{app} = 2.0 \cdot 10^{-1}$ M. The inset shows a plot of I_{ex} / I_{m1}.

suddenly decreased as shown in the inset of Figure 3-4. This result indicates that the encounter probability between the molecules in the excited and ground states decreased due to the increase of the microviscosity of the micelle at 4.8 h.

For the quantitative discussion of the microviscosity of the micelle, the fluorescence decay curve was observed. The rate equations at a subsequent time *t* after the excitation are given as follows.

$$\frac{d[M^*]}{dt} = -(k_a[M] + k_{01})[M^*] + k_d[D^*] \qquad (1)$$

$$\frac{d[D^*]}{dt} = k_a[M][M^*] - (k_d + k_{02})[D^*] \qquad (2)$$

where

$$k_{01} = k^f{}_{01} + k^n{}_{01} \qquad (3)$$

$$k_{02} = k^f{}_{02} + k^n{}_{02} \qquad (4)$$

Applying the boundary condition of $[M^*] = [M^*]_0$ and $[D^*] = 0$ at $t = 0$ and the assumption that the excimer dissociation is negligible compared to the deactivation rate of excimer ($k_{02} >> k_d$), the rise and decay curve of excimer emission is given as

$$[D^*] = \frac{k_a[M][M^*]_0}{k_{02} - (k_a[M] + k_{01})} \{e^{-(k_a[M]+k_{01})t} - e^{-k_{02}t}\} \qquad (5)$$

By analyzing the pyrene concentration dependence of the excimer decay, the value of k_a is evaluated according to eq. 5. Figure 3-5 shows the decay curves at $[Py]_{app} = 2.0 \cdot 10^{-1}$ M at the different elapse times. The decay curve was fitted successfully with the following equation.

$$I_D(t) = A_1(e^{-\frac{t}{\tau_\alpha}} - e^{-\frac{t}{\tau_\beta}}) \qquad (6)$$

The comparison between eqs. 5 and 6 leads to the following equation.

$$\frac{1}{\tau_\alpha} = k_a[M] + k_{01} \qquad (7)$$

According to eq. 7, a plot of $1/\tau_\alpha$ against the pyrene concentration $[M]$ is found to be linear and the slope corresponds to the value of k_a. Consequently, the pyrene

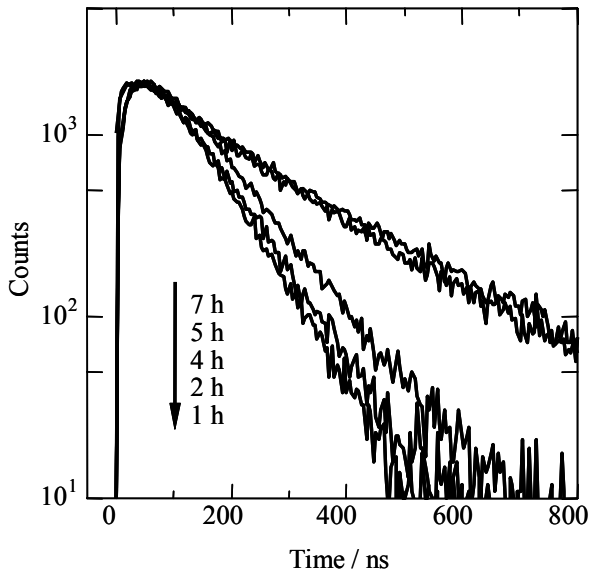

Figure 3-5. Excimer fluorescence decay after dispersing into water at $[Py]_{app} = 2.0 \cdot 10^{-1}$ M.

concentration [M] is important to estimate k_a. The pyrene molecules cannot exist uniformly in the micelle but locally in the hydrophobic core of WDPI micelle as mentioned above. Assuming that the HDIA forms the core of WDPI micelle and the density of HDIA and HDIA-MPEG is the same, the core volume is 54 % of the WDPI micelle. Therefore, the local pyrene concentration $[Py]_{local}$ can be estimated as the following equation.

$$[M] = [Py]_{local} = \frac{[Py]_{app}}{0.54} \qquad (8)$$

Figure 3-6 shows the linear relationship between $1/\tau_\alpha$ and $[Py]_{local}$. According to the Einstein-Stokes diffusion theory,[24-26] the rate of the excimer formation is given by

$$k_a = \frac{8RT}{3000\eta} \qquad (9)$$

where R, T and η are the ideal gas constant, the absolute temperature and the viscosity, respectively.[23, 27] Figure 3-7 indicates the microviscosity (η_{ex}) estimated from the value

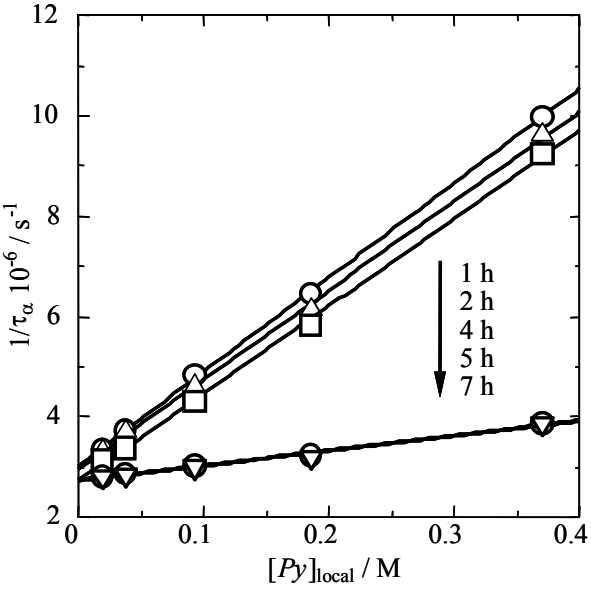

Figure 3-6. Plot of k_α against the local concentration of pyrene after dispersing into water.

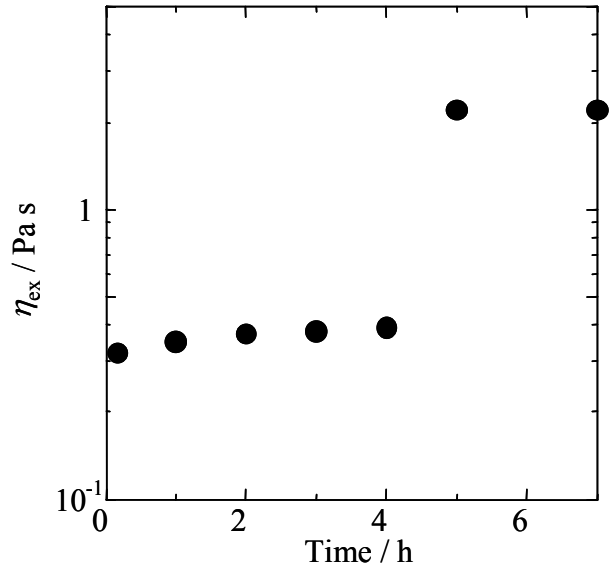

Figure 3-7. The microviscosity (η_{ex}) estimated from the rate of the excimer formation of pyrene.

of k_a according to the eq. 9. The η_{ex} remained almost constant until 4 h and suddenly increased between 4 and 5 h. This time range was equal to the induction period until the NCO group disappeared drastically. [18] The sudden reaction between the NCO groups of the WDPI and water molecules leads to the increase of the microviscosity in the micelle.

3.3.3. Microviscosity of WDPI Micelle Estimated by Fluorescence Depolarization of Perylene

The fluorescence depolarization occurs by the rotational motion of the excited fluorescent molecule, so that fluorescence anisotropy reflects the microviscosity around the fluorescence molecule. The fluorescence anisotropy, r, is defined as

$$r = \frac{I_{//} - GI_{\perp}}{I_{//} + 2GI_{\perp}} \qquad (10)$$

where $I_{//}$ and $I\perp$ are the observed polarized components parallel and perpendicular to the polarization direction of the excitation beam, respectively, and G is the instrumental correlation factor to compensate the different detection sensitivity for $I_{//}$ and $I\perp$. The value of r_0 / r observed by the steady state excitation is an index of the rotational

diffusion during the lifetime of the excited state, where r_0 is the limiting fluorescence anisotropy obtained without the rotational motion. The r_0 / r is related to the viscosity of the medium (η) by the Perrin equation

$$\frac{r_0}{r} = 1 + \frac{kT\tau}{V\eta} \qquad (11)$$

where k is the Boltzmann constant, V is the molecular volume, and τ is the fluorescence lifetime of perylene. The lifetime of perylene in the WDPIs at 298 K was measured as 5.0 ns. Figure 3-8 shows that the relation between $1/r$ and $1/\eta$ is derived from the measured r of perylene in some WDPI medium with known viscosities. From this figure, r_0 and V can be estimated from the intercept and the slope. Assumingthat r_0 and V are the same in both WDPI solution and the inside the micelle, the microviscosity (η_{dep}) of the WDPI micelle was estimated by using the parameters obtained. Figure 3-9 shows the value of η_{dep} as a function of the elapsed time after dispersing.

The η_{dep} also gradually increased until 4 h and drastically increased between 4.5

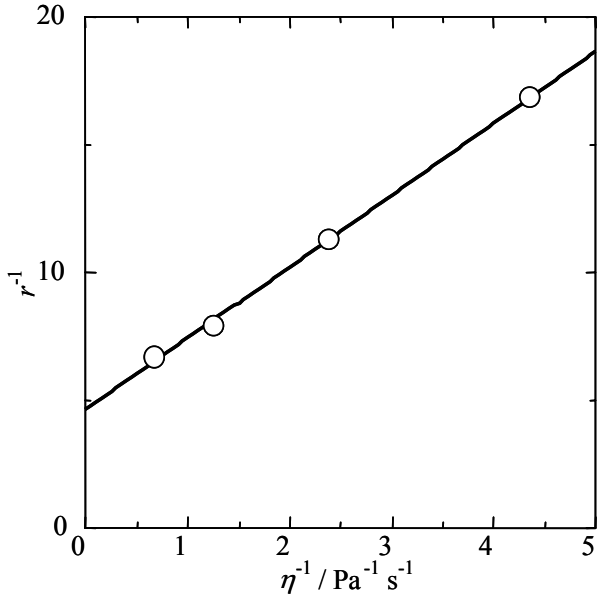

Figure 3-8. Perrin plot for the MPEG modified HDI derivatives with different viscosity.

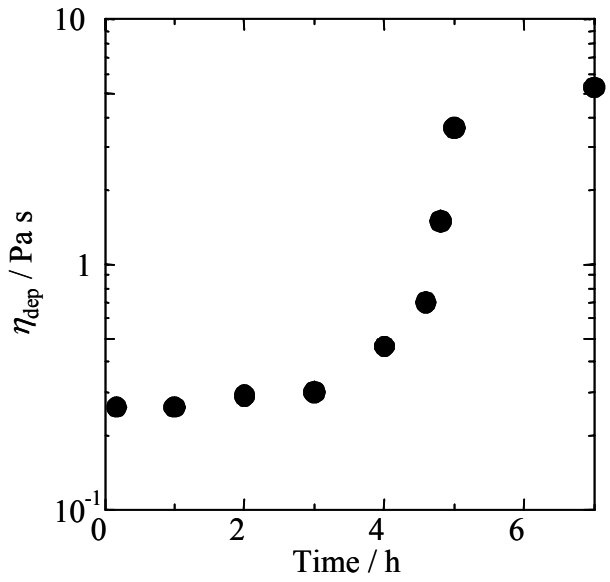

Figure 3-9. The microviscosity (η_{dep}) estimated from the fluorescence depolarization of perylene.

and 5 h. That is, the results by the fluorescence depolarization measurement also indicate that the reaction between the NCO groups of WDPI and water molecules proceeds inside the micelle and the intermolecular polymerization causes the drastic increase of the microviscosity.

3.4. Conclusion

The microviscosity of the WDPI micelle was quantitatively estimated by the two fluorescence techniques; the excimer formation rate and the fluorescence depolarization revealed the translational and rotational diffusivities in the interior of micelles, respectively. The fluorescent dyes existed in the core of the WDPI micelle locally due to their hydrophobicities, therefore, they reflect the internal state of the WDPI micelle. The microviscosity change of the WDPI micelle showed that the NCO groups of the WDPI were retained in the core of micelles for ca. 4 h, and then the sudden polymerization after the induction period led to the drastic increase of microviscosity of WDPI micelle.

The increase of the microviscosity decreases the wettability of the WDPI droplet onto the substrate and interfere the fusion of the droplets to form the film, resulting in the decrease of the adhesiveness and the strength of the uniform film. These results indicate that the microviscosity of the individual micelle is an important factor on determining the practical performance of the waterborne coating system.

References

1. T. Förster, and B. K. Selinger, *Z. Naturforsch*, **19A**, 38 (1964)

2. H. J. Pownall, and L. C. Smith, *J. Am. Chem. Soc.*, **95**, 3136 (1973)

3. K. A. Zachariasse, *Chem. Phys. Lett.*, **57**, 429 (1978)

4. J. Emert, C. Behrens, and M. J. Goldenberg, *J. Am. Chem. Soc.*, **101**, 771 (1979)

5. N. J. Turro, M. Aikawa, and A. Yekta, *J. Am. Chem. Soc.*, **101**, 772 (1979)

6. N. J. Turro, and T. Okubo, *J. Am. Chem. Soc.*, **103**, 7224 (1981)

7. W. D. Turley, and H. W. Offen, *J. Phys. Chem.*, **89**, 2933 (1985)

8. R. Zana, *J. Phys. Chem. B*, **103**, 9117 (1999)

9. M. Bradley, M. Ashokkumar, and F. Grieser, *J. Am. Chem. Soc.*, **125**, 525 (2003)

10. M. Shinitzky, A. C. Dianoux, C. Gitler, and G. Weber, *Biochem.*, **10**, 2106 (1971)

11. M. Grätzel, and J. K. Thomas, *J. Am. Chem. Soc.*, **95**, 6885 (1973)

12. M. McCarroll, K. Toerne, and R. Wandruszka, *Langmuir*, **14**, 2965 (1998)

13. S. Matzinger, D. M. Hussey, and M. D. Fayer, *J. Phys. Chem. B*, **102**, 7216 (1998)

14. C. C. Ruiz, *J. Colloid Interface Sci.*, **221**, 262 (2000)

15. G. B. Dutt, *J. Phys. Chem. B*, **108**, 3651 (2004)

16. J. W. Borst, M. A. Hink, A. Hoek, and A. J. W. G. Visser, *J. Lumin.*, **15**, 153 (2005)

17. G. Kamaromy-Hiller, and R. Wandruszka, *J. Colloid Interface Sci.*, **221**, 262 (1996)

18. F. G. Sanchez, and C. C. Ruiz, *J. Lumin.*, **69**, 179 (1996)

19. A. Nakajima, *Bull. Chem. Soc. Jpn.*, **44**, 3272 (1971)

20. K. Kalyanasundaram, and J. K. Thomas, *J. Am. Chem. Soc.*, **99**, 2039 (1977)

21. C. Honda, M. Itagaki, R. Takeda, and K. Endo, *Langmuir*, **18**, 1999 (2002)

22. J. B. Birks, D. J. Dyson, and I. H. Munro, *Proc. Roy. Soc. Ser. A*, **275**, 575 (1963)

23. J. B. Birks, Photophysics of aromatic molecules. A Wiley-Interscience Publication, New York (1970)

24. P. Debye, *Trans. Electrochem. Soc.*, **82**, 205 (1942)

25. J. Q. Umberger, and V. K. LaMer, *J. Am. Chem. Soc.*, **67**, 1099 (1945)

26. R. M. Noyes, *Progr. React. Kinet.*, **1**, 131 (1961)

27. J. B. Birks, *Rep. Prog. Phys.*, **38**, 903 (1975)

Chapter 4

Colloidal Characteristics and Film Properties of Waterborne Two-Component Polyurethanes

4.1. Introduction

The polyurethane coating system is classified into the two major categories of the one-component (1K) and two-component (2K) systems. In the 1K system, the high molecular weight polyurethane is coated on a substrate from the solution and the solid film is formed by the solvent evaporation. The 1K system has achieved high performance; but it has some defects such as the lack of solvent resistance due to the linear structure of the polyurethane. On the other hand, the 2K system consists of two kinds of polymers: the polyol component with an OH group and the polyisocyanate component with a NCO group. They are mixed and coated on a substrate to form the film. In the film forming and curing processes, the reaction between polyol and polyisocyanate yields the crosslinked high molecular weight polyurethane film. Concerning the coating performance such as solvent durability and adhesiveness, the 2K system is useful to form a tough film by the crosslinking reaction after coating.

In recent years, the reduction of volatile organic compounds (VOCs) is in strong demand and waterborne (WB) PU is now one of the most attractive materials. [1-8] Therefore, it stands to reason that the WB 2K-PU system has been widely introduced since the 1990 when water-dispersible polyisocyanate (WDPI) was developed by

modifying polyisocyanate with hydrophilic methoxy polyethylene glycol (MPEG), which allowed one to achieve both the performance of solventborne 2K-PU systems and the reduction of VOCs. [11-17] The basic WB 2K-PU system consists of acrylic, polyester or polyurethane dispersion (PUD) with a hydroxy-functional group and WDPI. These components are easily mixed by stirring and form a stable aqueous dispersion with a low viscosity. Although the large advantage of the WB 2K-PU system has put it to practical use in the last decade, only a few fundamental studies have been reported. For example, Jürgens et al. [9] investigated the reaction, film formation and drying process in WB 2K-PU systems consisting of hydroxyfunctional polyacrylate dispersion and WDPI. Urban et al. [10-14] showed that the film morphology of WB 2K-PU systems consisting of polyester dispersion and WDPI depended on different curing and mixing conditions. These studies pointed out that WB 2K-PU systems are highly sensitive to environmental and process conditions, such as temperature, humidity and shear history.

The largest difference between WB and solventborne 2K-PU system is the medium, water or organic solvent. The existence of water around the NCO groups makes it difficult to understand the WB 2K-PU system due to the high reactivity of NCO groups to water molecules. In the WB 2K-PU system, the intermicellar reaction between the NCO group of WDPI and the hydroxyfunctional dispersions and the side reaction between that of WDPI and water molecules are competitive. Therefore, the time after mixing WDPI with PUD (TAM) is important on determining the colloidal characteristics and the properties of the resulting films. In order to examine the effect of TAM on the film, hydroxyfunctional PUD and WDPI labeled with Rhodamine B were prepared. The reaction of WDPI in colloidal state was evaluated by the particle size distribution, titration and GPC measurement, and the properties of the film obtained

with the WB 2K-PU system were investigated by the stress-strain (s-s) curves, the viscoelasitic properties and the fluorescence microscope image. On directly observation of the film morphology by fluorescent microscopy, the WDPI labeled with Rhodamine B is very useful due to the high fluorescence quantum yield of Rhodamine. [15-17] The objective of Chapter 4 is to clarify the relations among the reaction in the colloidal state, the film morphology and the physical properties of the film obtained with the WB 2K-PU system.

4.2. Experimental Section

4.2.1. Materials

Polycarbonatediol (PCD) with a molecular weight of 2000 (Asahi Kasei Industries Ltd.) was dried at 80 ˚C for 3 h under nitrogen bubbling before use. Rhodamine B isothiocyanate (RBITC) (Sigma-Aldrich) and 2-2-bis(hydroxymethyl)propionic acid (DMPA) (Nippon Kasei Chemical) were used without further purification. 3-Isocyanatomethyl-3,5,5-triethylcyclohexyl isocyanate (IPDI), triethylamine (TEA), 2-(2-aminoethylamino)ethanol, 1-hexanol, 2-amino-2-methyl-1,3-propanediol (AMPD), and dibuthyltin(IV) dilaurate (DBTDL) were received from Wako Pure Chemical Industries, Ltd.. These materials were used as received.

4.2.2. PUD Preparation

A 500 mL round-bottom four-necked flask equipped with a stirrer, thermometer, nitrogen inlet, and a condenser was used as a reactor. IPDI (51.9 g, $2.3 \cdot 10^{-1}$ mol) and acetonitrile (45.0 g) were charged into the dried flask. Under nitrogen atmosphere, DMPA (14.3 g, $1.1 \cdot 10^{-1}$ mol) and 1-hexanol (0.15g, $1.4 \cdot 10^{-3}$ mol) were added while

stirring and the mixture was heated to 70 ˚C. After 1 h, DBTDL (42.0 mg) was added as a catalyst. The reaction was carried out at 70 ˚C for 3 h with stirring. The NCO content during the reaction was determined using the dibuthylamine back-titration method (ASTM D 1638). Upon obtaining a theoretical NCO value, PCD (Mn = 2,000, 95.6 g, $4.8 \cdot 10^{-2}$ mol) and acetonitrile (30.0 g) were added and the polymerization reaction was carried out for 6 h at 70 ˚C until reaching the theoretical NCO content. And then, the reaction solution (prepolymer) was cooled to 30 ˚C and neutralized with TEA (10.8 g, $1.1 \cdot 10^{-1}$ mol). The stoichiometric ratio of TEA to COOH was 1.0. After neutralizing reaction, the prepolymer solution (206 g) was poured into the distilled water (350 g) under the constant agitation (2,000 rpm) at 20˚C. The stable dispersion is formed at this stage and the dispersion with the reactive NCO groups was extended by adding a 10 wt % aqueous solution of 2-(2-aminoethylamino)ethanol (39.3 g, $3.8 \cdot 10^{-2}$ mol). The chain extension reaction was carried out for the next 1 h under the same agitation condition. The stoichiometric ratio of the amine group of 2-(2-aminoethylamino)ethanol to the NCO group of the prepolymer was 0.9. After the residual acetonitrile was reduced by the rotary evaporation, PUD (30 wt % concentration) was obtained. The OH group content for the PUD solid is $2.5 \cdot 10^{-1}$ mmol / g.

4.2.3. Labeling of WDPI

Hexamethylene diisocyanate (HDI) allophanate and WDPI were synthesized as described in Chapter 2. WDPI was labeled with RBITC according to Scheme 4-1. In the first step, RBITC (51.1 mg, $9.5 \cdot 10^{-5}$ mol) dissolved in chloroform (5.0 g) was reacted with AMPD (10 mg, $9.5 \cdot 10^{-5}$ mol) at 40 ˚C for 4 h. The reaction product (**I**) was precipitated in hexane three times and dried. In the second step, IPDI (87 mg, $3.9 \cdot 10^{-4}$

Scheme 4-1. Labeling process of the WDPI

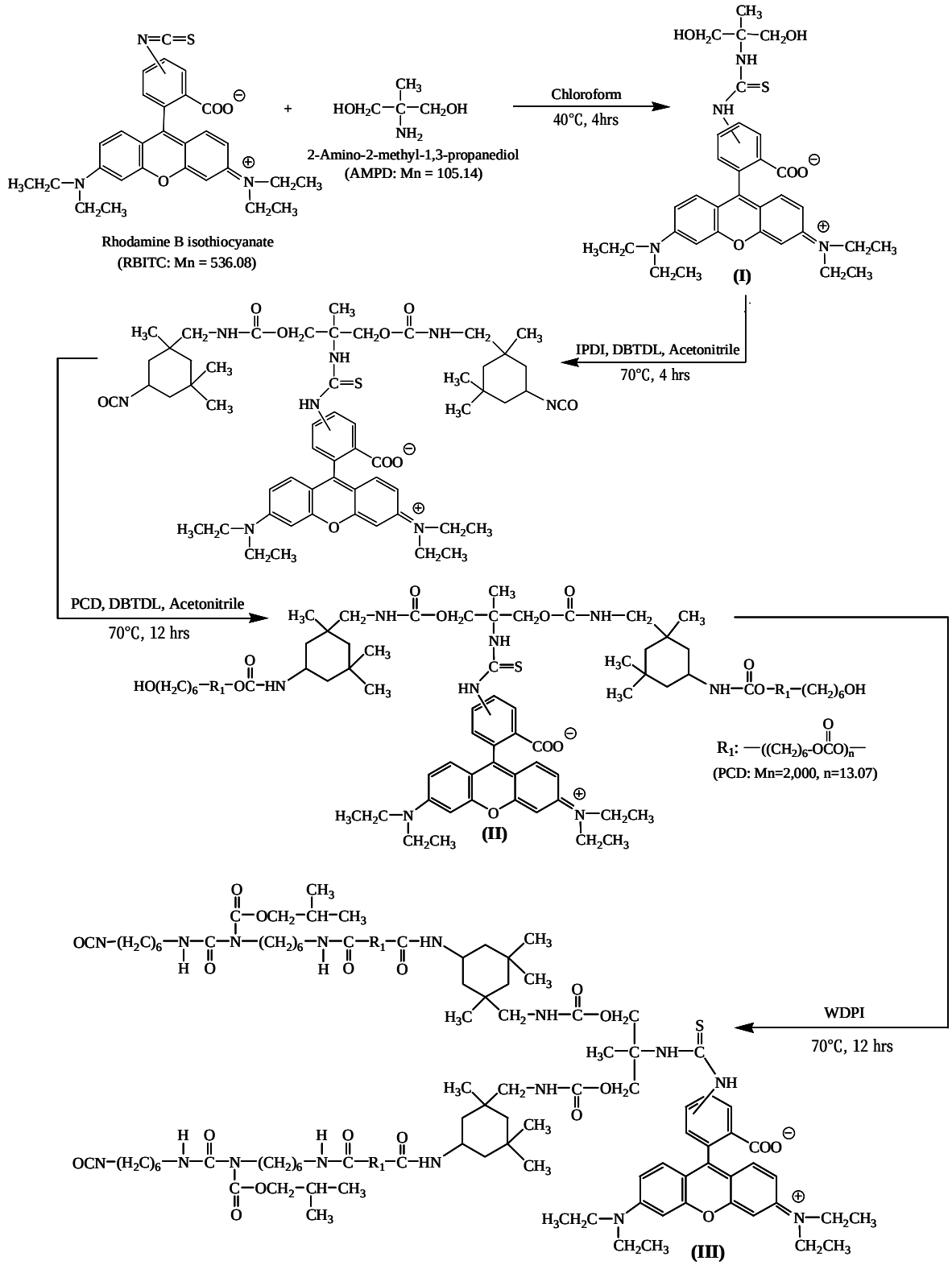

mol) dissolved in acetonitrile (0.12 g) was reacted with the product (**I**) (50 mg). The reaction was catalyzed by DBTDL ($2.3 \cdot 10^{-2}$ mg) and carried out at 70 ˚C for 5 h. Continuously, PCD (6.2 g, $3.1 \cdot 10^{-3}$ mol), acetonitorile (6.2 g) and DBTDL (1.2 mg) were added to the solution, which was the kept at 70 ˚C for 12 h. The reaction product (**II**) was precipitated in methanol three times and thoroughly washed with ethanol to remove free dye. In the third step, the product (**II**) (17 mg) was added to the HDI allophanate (1.7 g), and the reaction was carried out at 70 ˚C for 12 h to obtain the product (**III**). The labeled WDPI was prepared by mixing the product **III** (50 mg) with WDPI (5.0 g) for 3 h. Rhodamine B and the NCO group content of WDPI were estimated to be $2.0 \cdot 10^{-7}$ and 3.1 mmol / g by the absorption spectrum and titration, respectively. The specific gravity of WDPI is 1.09.

4.2.4. WB 2K-PU Dispersion

WDPI (1.2 g) was poured into the distilled water (2.8 g) with stirring and kept stirred for 10 min. Into the stable WDPI dispersion thus obtained, PUD was added and mixed under the same stirring condition for another 10 min. The stoichiometric ratio of the NCO group of WDPI to the OH group of PUD was 2.0, and the concentration of the WB 2K-PU system was 30 wt%. After the mixing, it was held without stirring and a part of it was collected at a certain TAM. TAM is defined as the elapsed time after the mixing of PUD.

4.2.5. Film Formation

Film samples were prepared by casting the WB 2K-PU dispersion at TAM = 1 h, 4 h, and 8 h on glass Petri dishes under ambient temperature. The film was crosslinked for

3 days at ambient temperature in the desiccator (dry condition) and completely cured at 110 ˚C for 1 h. The film thickness was ca. 60 μm.

4.2.6. Measurements

Particle size distribution was measured by the dynamic light scattering (DLS) with a Beckman Coulter N5 submicron particle size analyzer at ambient temperature. Prior to the particle size measurement, the samples were diluted to the required concentration with distilled water.

NCO contents of the WB 2K-PU dispersion were measured by the dibutylamine backtitration method when the WB 2K-PU dispersion was sampled at a certain TAM.

Molecular weight was determined by GPC measurements (HITACHI D-7000G) in THF. GPC was calibrated with monodisperse polystylene standards, Mn = $1.67 \cdot 10^4$, $4.28 \cdot 10^4$ and $1.07 \cdot 10^5$.

Mechanical properties were measured at 25 ˚C using INTESCO Model 205 following the ASTM D-412 specifications. A crosshead speed was 50 mm/min. The values quoted are the average of five measurements.

Viscoelasitc properties were measured at 10 Hz using DVA-200 instrument (IT Keisokuseigyo) at a heating rate of 5 ˚C / min in the temperature range from -100 to 200 ˚C.

The morphological observation of the film formed from the WB 2K-PU dispersion was made with a fluorescence microscope (NIKON ECLIPSE TE2000-E).

4.3. Results and Discussion

4.3.1. Colloidal Characteristics

Figure 4-1 shows the chemical structures of PUD and WDPI composing the WB

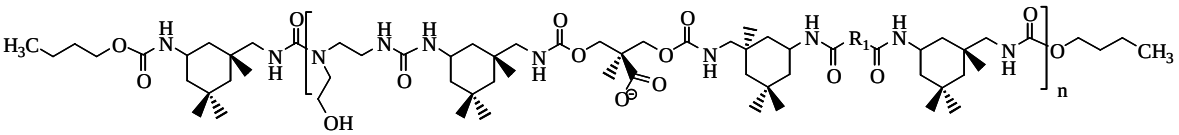

Polyurethane Dispersion (PUD)

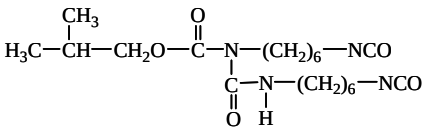

HDI Allophanate

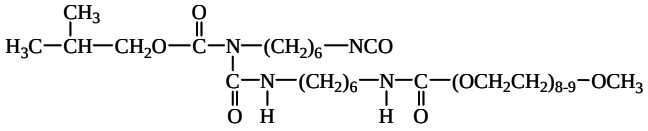

HDI Allophanate Modified with MPEG

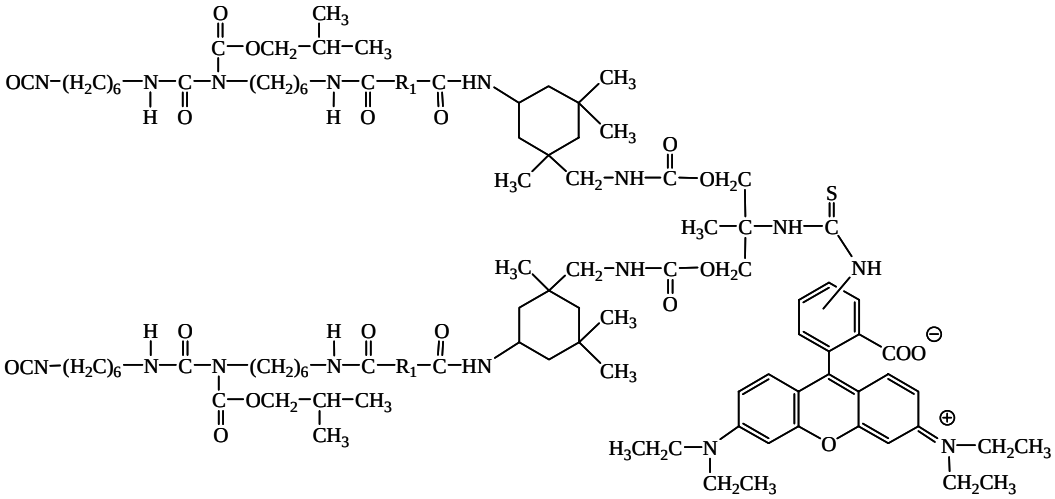

HDI Allophanate Labeled with Rhodamine

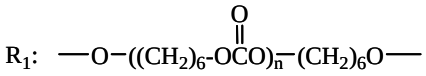

Polycarbonatediol
(PCD: Mn=2,000, n=13.07)

Water-Dispersible Polyisocyanate Labeled with Rhodamine B (WDPI)

Figure 4-1. Chemical structures for WB 2K-PU compounds.

2K-PU system. The PUD backbone contains pendant carboxyl groups, which are neutralized with triethylamine. The amine salts give the PU backbone significant hydrophilicity, resulting in the small and narrow distribution of the particle size as shown in Figure 4-2. In contrast, WDPI is a complicated material, consisting of a mixture of hydrophobic HDI allophanate, the hydrophilic HDI allophanate modified with MPEG, and a very small amount of the hydrophobic HDI allophanate labeled with

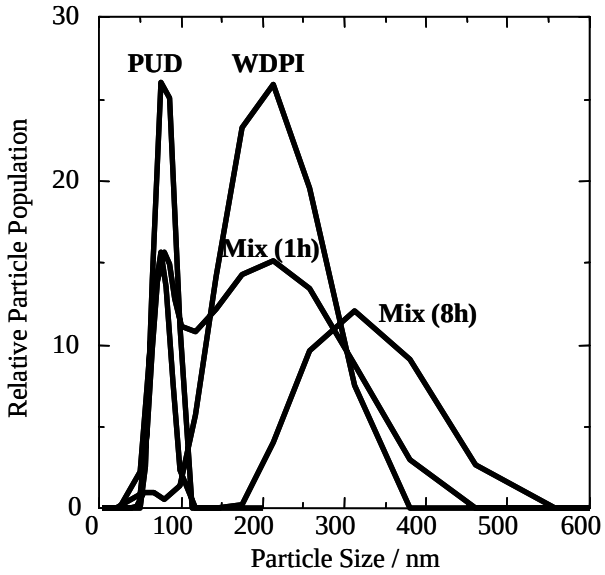

Figure 4-2. Particle size distribution of PUD, WDPI and WB 2K-PU reactive dispersion with NCO : OH = 2.0 at 1 h and 8 h after mixing.

Rhodamine B, as shown in Figure 4-1. Upon using appropriate shearing conditions, the WDPI forms a stable aqueous dispersion, where the hydrophilic isocyanate is located around the periphery of the hydrophobic isocyanate droplets. However, the emulsifying ability of the non-ionic group of the WDPI is presumed to be weaker than the amine salt of PUD, resulting in the large average diameter (200 nm) and the wide distribution of the particle size.

Figure 4-2 also shows the change of the particle size distribution of the WB 2K-PU system with TAM. After a short TAM, the two separate peaks derived from the PUD and the WDPI micelles indicate that each droplet of PUD and WDPI exists independently in aqueous medium. Larger particle size droplets gradually increased with TAM.

In a 2K-PU system, the content of the reactive NCO groups in the colloidal state is important for the cross-linking structure of the obtained film and the adhesiveness to the substrate. Especially in the WB 2K-PU system, the NCO group is so reactive that side

reactions occur with the carboxyl groups of PUD and with water, as well as the desired cross-linking reaction with the OH group of PUD. Figure 4-3 shows that the reactions of the NCO group in the WB 2K-PU system. In these reactions, the reactivity of the carboxyl group of PUD is extremely low because of the neutralized form in dispersion state, although the carboxyl groups have similar reactivity to the OH groups once the amine neutralization agent leaves the carboxyl unit. Figure 4-4 shows the residual NCO contents of the WB 2K-PU system (solid line) and the WDPI without PUD (broken line) in the colloidal state water. The WB 2K-PU system showed steady decrease of the NCO content with TAM. In contrast, the NCO content of aqueous WDPI dispersion without PUD suddenly decreased after an induction period. This sudden reaction between NCO and water was due to the core-shell structure of WDPI in water medium; the shell is the hydrophilic HDI allophanate with MPEG and the core is the hydrophobic HDI allophanate without MPEG.[14] Therefore, the large NCO consumption at a short TAM in

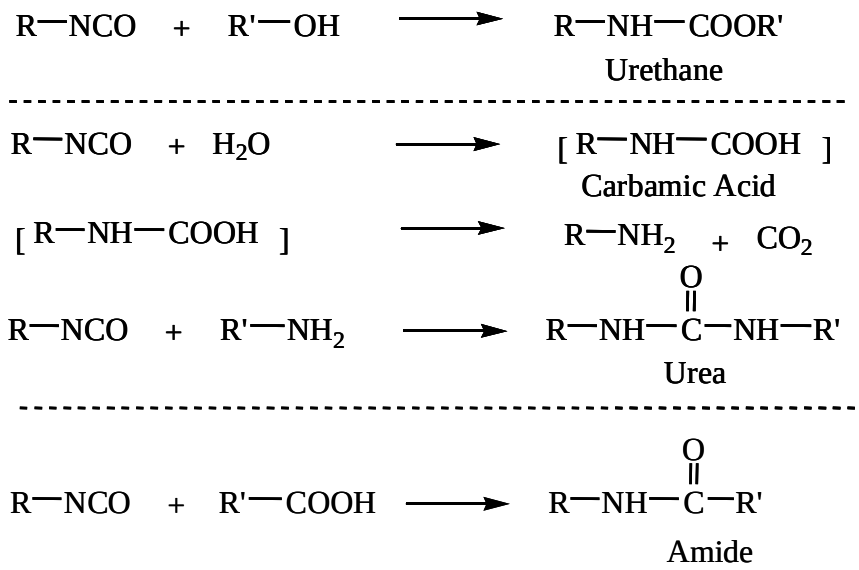

Figure 4-3. NCO reactions with OH, water and carboxylic group.

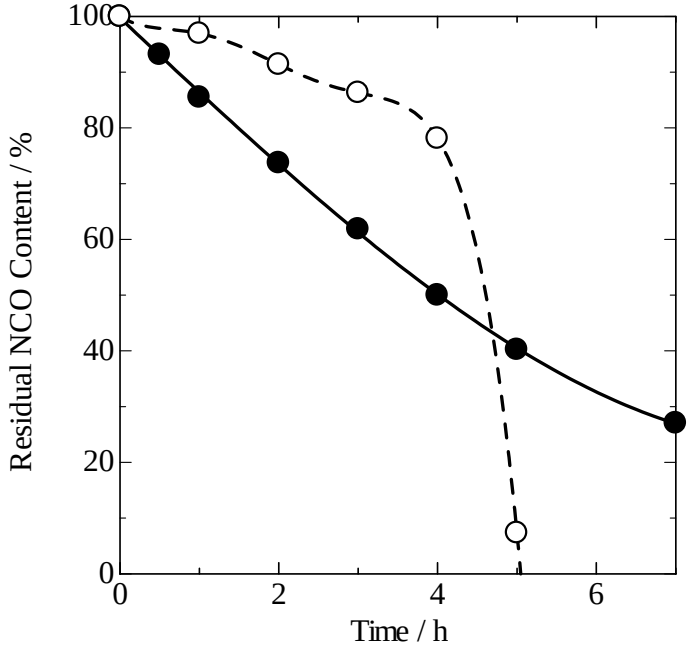

Figure 4-4. Residual NCO content of the WB 2K-PU reactive dispersions as a function of TAM.

the WB 2K-PU system indicates the effective introduction of PUDs into the core-shell structure of WDPI and the progress of reaction between the NCO groups in the core and the OH groups of PUD.

For the quantitative discussion on the NCO reaction of WDPI, the molecular weight of the WB 2K-PU system was measured. The GPC curve (the inset of Figure 4-5) shows two separate peaks; Mw-H and Mw-L are attributed to the molecular weights of PUD and WDPI, respectively. Both the Mw-H and Mw-L gradually increase with TAM, because the intermicellar reaction between PUD and WDPI droplets results in the increase of the Mw-H, and the side reaction between WDPI and water molecules yields the increase of the Mw-L. From the increase of Mw-H and Mw-L, the ratio of the number of the NCO groups reacting with the OH groups of PUD and with the water

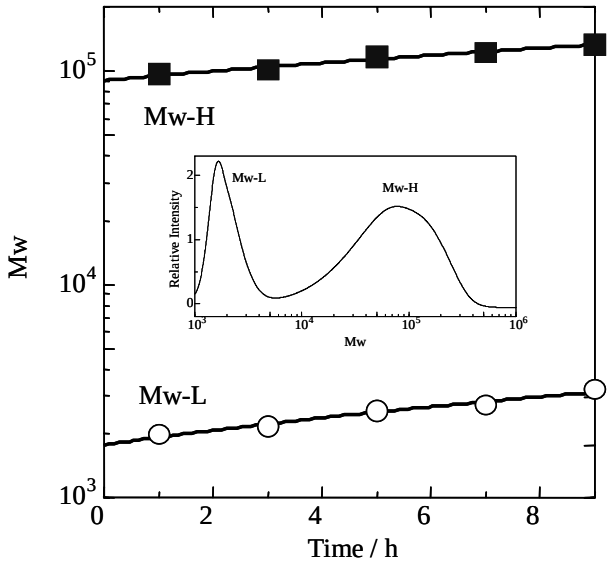

Figure 4-5. Molecular weight of PUD and WDPI as a function of TAM.

molecules can be estimated as 1 : 5, assuming that the NCO groups of WDPI undergo intermolecular reactions mainly with the OH groups of PUD and with the hydrolytic product of WDPI. The ratio 1 : 5 indicates that the NCO groups of WDPI preferentially react with the OH groups of PUD, considering that the stoichiometric ratio of NCO to the OH group in the WB 2K-PU system is only 2.0, while a relatively large amount of water molecules present around the WDPI droplets. The preferential reaction with PUDs results in coalescence of micelles as illustrated in Figure 4-6C_1 and C_2. When WDPI is dispersed into water, it forms the core-shell structure; the hydrophilic HDI allophanate modified with MPEG is present in the shell part and the hydrophobic HDI allophanate without MPEG is in the core part of the micelle, as shown in Figure 4-6A. Similarly, the hydrophilic groups like the carboxyl and hydroxyl groups of PUD are favorably located at the periphery of the micelle as shown in Figure 4-6B. Figure 4-6C_1 depicts the WB 2K-PU system at a short TAM. When the PUD contacts with the WDPI

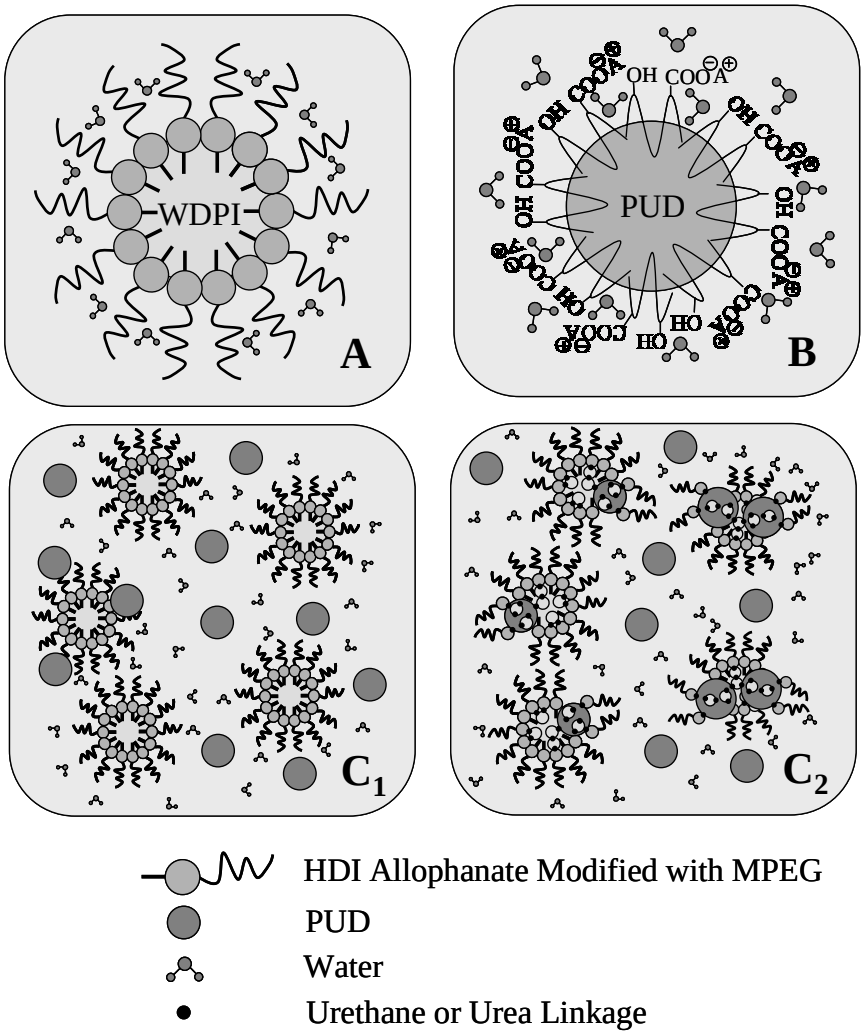

Figure 4-6. Schematic illustration of WB 2K-PU system.
A: WDPI aqueous dispersion.
B. PUD.
C_1, C_2. WB 2K-PU system.

droplets, the OH groups at the periphery of PUD easily react with the NCO groups of WDPI, because the primary OH groups are more reactive to the NCO group than the water molecules. With TAM, the reaction between the OH groups of PUD and the NCO groups of WDPI proceeds, resulting in the increase of both the molecular weight of polymers and the size of WDPI droplets, as shown in Figure 4-6C_2. The large size of the

micelle and the hydrophobicity inside the micelle prevent the water molecules from invading into the micelle.

4.3.2. Film Properties

In this section, the physical property and the morphology of film prepared with the WB 2K-PU system at different TAM are examined. Figure 4-7 shows the storage modulus *E'* as a function of temperature. At different TAMs, the curves of the storage modulus hardly change and show the plateau from 30 to 170 ˚C. It is well-known that the *E'* curves in the rubbery state at a high temperature strongly depend on the molecular weight of polymers because of the presence of chain entanglement. The very similar feature of *E'* curves in Figure 4-7 shows that the major part of films after complete curing are composed of polymers with the same molecular weight. However,

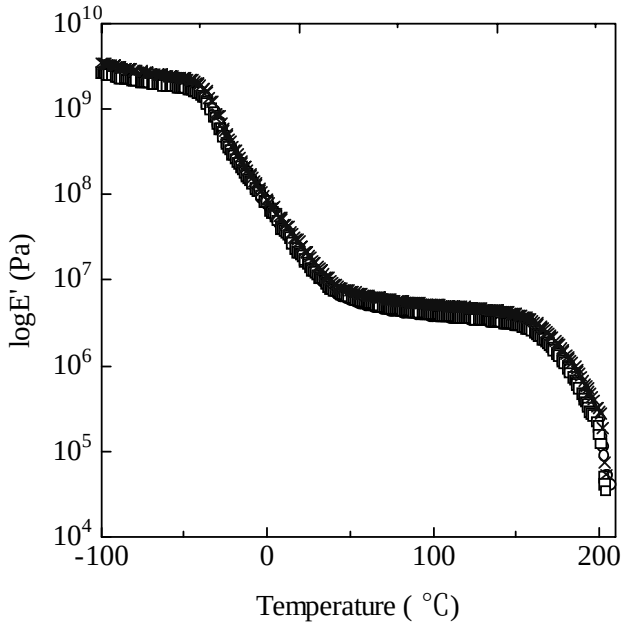

Figure 4-7. Storage modulus (E') as functions of temperature for the WB 2K-PU films at different TAM: (○) 1 h, (□) 4 h and (×) 8 h.

the stress-strain curves in Figure 4-8 show that the stresses at the break drastically decrease with TAM. The fluorescence images of the films explain the reason of the difference of the stress at the break. Figure 4-9 shows the micrographs of the films prepared at different TAMs. The micrographs indicate the significant morphological changes; the film is uniformly luminous immediately after mixing, the bright spots begin to appear at 1 h, and the bright spots become larger with TAM. The bright spot is the emission from WDPI labeled with Rhodamine B, accordingly, the bright domain includes a large number of the WDPI. The change of the morphology is caused primarily by the compounds produced by the intermolecular reaction between PUD and WDPI. The differences of the film formation with TAM are illustrated in Figure 4-10. Immediately after mixing, the WB 2K-PU system consists of only PUD and WDPI, which are compatible and form a homogeneous film. With TAM, the NCO groups of WDPI react with the OH groups of PUD and water molecules in the colloidal state. Among the reaction products, the compound that reacted between PUD and WDPI has a very high molecular weight, resulting in low compatibility and it easily aggregated during film formation. The increase of size with TAM facilitates the phase separation and large domains are formed. The stress and strain of the obtained film depend on the domain size. The strength of the boundary between the domains is weak due to the immiscibility and incompatibility. The weak interface in the film allows easy crack propagation, resulting in the decrease of the elongation and the tensile strength at break.

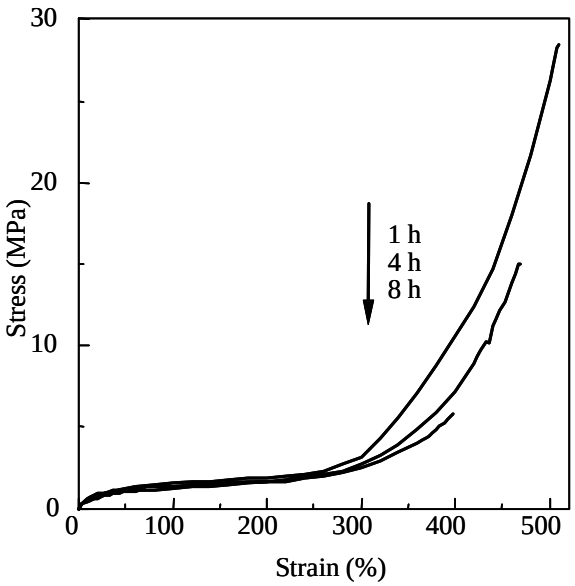

Figure 4-8. Stress-strain curves of the WB 2K-PU films at different TAM: (◯) 1 h, (□) 4 h and (✕) 8 h.

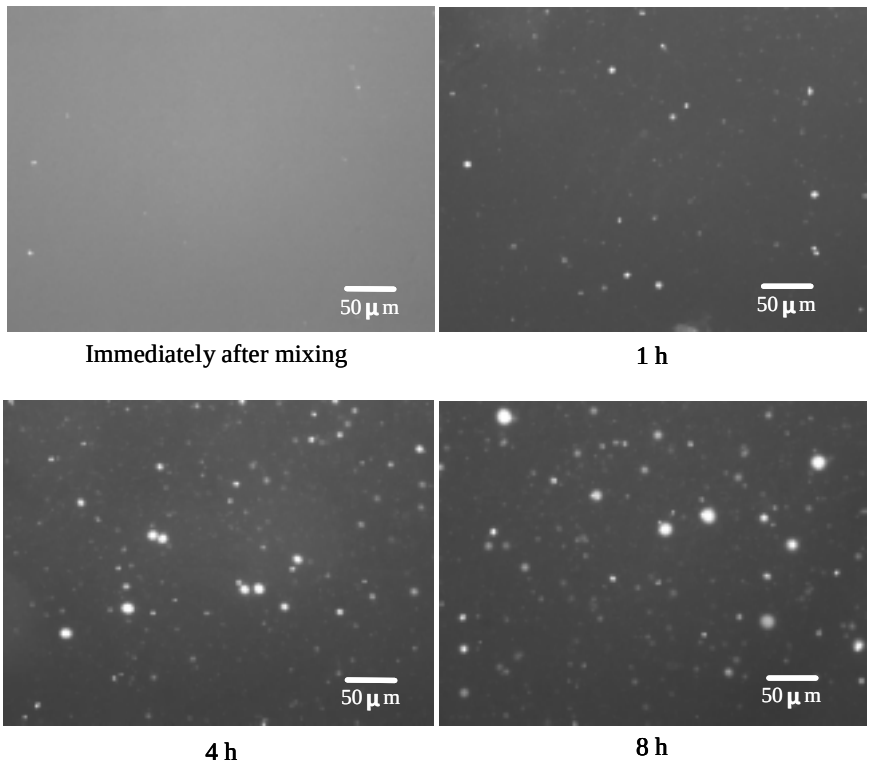

Figure 4-9. Fluorescence micrograph of the WB 2K-PU films at different TAM: immediately after mixing, 1 h, 4 h and 8 h.

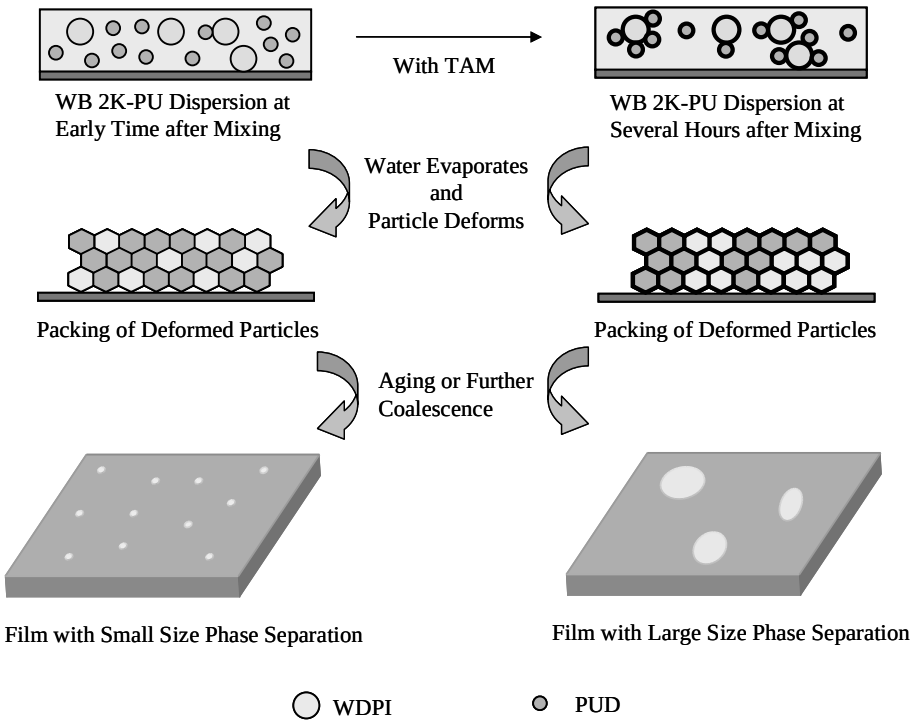

Figure 4-10. Schematic illustration of the film formed from the WB 2K-PU system with TAM.

4.4. Conclusion

In the WB 2K-PU system, the inter-micellar reaction in aqueous dispersion was examined in relation to the morphology and the physical properties of the resulting film. From the evaluation of particle size, molecular weight, and NCO content, the inter-micellar reaction between PUD and WDPI proceeds preferentially in the colloidal state due to the location and the high reactivity of the OH groups of PUD. The film morphology was drastically changed with TAM. The changes were mainly caused by the increase of the polymers produced by the intermolecular reaction between PUD and WDPI with TAM. They aggregate and form a phase-separated structure because of the incompatibility due to the outstanding high molecular weight. The progression of the phase separation resulted in the decrease of the mechanical strength of the obtained film,

because the boundary worked as a weak point to break the film. These fundamental data allowed us to interpret for the first time the reaction process of WB 2K-PU systems, and revealed the origin of the drastic decrease in mechanical strength as a result of the progression of phase separation.

References

1. D. Dieterich, *Prog. Org. Coat.*, **9**, 281 (1981)

2 B. K. Kim, T. K. Kim, and H. M. Jeong, *J. Appl. Polym. Sci.*, **53**, 371 (1994)

3. S. Zhang, L. Cheng, and J. Hu, *J. Appl. Polym. Sci.*, **90**, 257 (2003)

4. T. Tawa, and S. Ito, *Polym. J.*, **38**, 686 (2006)

5. I. Soutar, L. Swanson, T. Annable, J. C. Padget, and R. Satgurunathan, *Langmuir*, **22**, 5904 (2006)

6. S. A. Madbouly, J. U. Otaigbe, A. K. Nanda, and D. A. Wicks, *Macromolecules*, **38**, 4014 (2005)

7. P. Król, B. Król, P. Holler, and N. Telitsyna, Colloid Polym. Sci., **284**, 1107 (2006)

8. Z. W. Wicks, Jr., D. A. Wicks, and J. W. Rosthauser, *Prog. Org. Coat*., **44**, 161 (2002)

9. M. Melchiors, M. Sonntag, C. Kobusch, E. Jürgens, *Prog. Org. Coat*., **40**, 99 (2000)

10. P. B. Pandey, and M. W. Urban, *Langmuir*, **20**, 2970 (2004)

11. D. B. Otts, L. A. Cueva-Parra, R. B. Pandey, and M. W. Urban, *Langmuir*, **21**, 4034 (2005)

12. D. B. Otts, and M. W. Urban, *Polymer*, **46**, 2699 (2005)

13. D. B. Otts, K. J. Pereira, W. L. Jarret, and M. W. Urban, *Polymer*, **46**, 4776 (2005)

14. T. Tawa, and S. Ito, *Colloid Polym. Sci*., **283**, 781 (2005)

15. K. K. Rohatgi, and G. S. Singhal, *J. Phys. Chem.*, 67, 2844 (1963)

16. P. J. Sadkowski, and G. R. Fleming, *Chem. Phys. Lett*., **57**, 526 (1978)

17. I. L. Arbeloa, and P. R. Ojeda, *Chem. Phys. Lett.*, **79**, 347 (1981)

Part II

Chapter 5

The Role of Hard Segments of Aqueous Polyurethane-Urea Dispersion in Determining the Colloidal Characteristics and Physical Properties

5.1. Introduction

Polyurethane is a unique polymeric material with a wide range of physical and chemical properties. The properties of polyurethane originate from the microphase separation structure in polyurethane films because the polyurethane chain consists of soft and hard segments as shown in Figure 5-1. A hard domain formed by hydrogen bonding of hard segments provides properties of both physical crosslinkage and filler-like reinforcement. [1-7]

Recently, aqueous polyurethane-urea dispersion (PUD) is gathering considerable attention due to the growing concern to preserve the environment. [8-15] PUD can be prepared by introducing ionic moieties into a polyurethane, neutralizing and then dispersing them into water if a sufficient amount of the ionic moiety is incorporated. The presence of an ionic group in the hard segment has a considerable effect on its physical properties and it is reasonable to suppose that the interaction between acid groups and their counterions is responsible for these effects. The degree of neutralization, [16-19] the type of counterion, [20-24] and the amount of ionic compound [25, 26] significantly influence the physical properties.

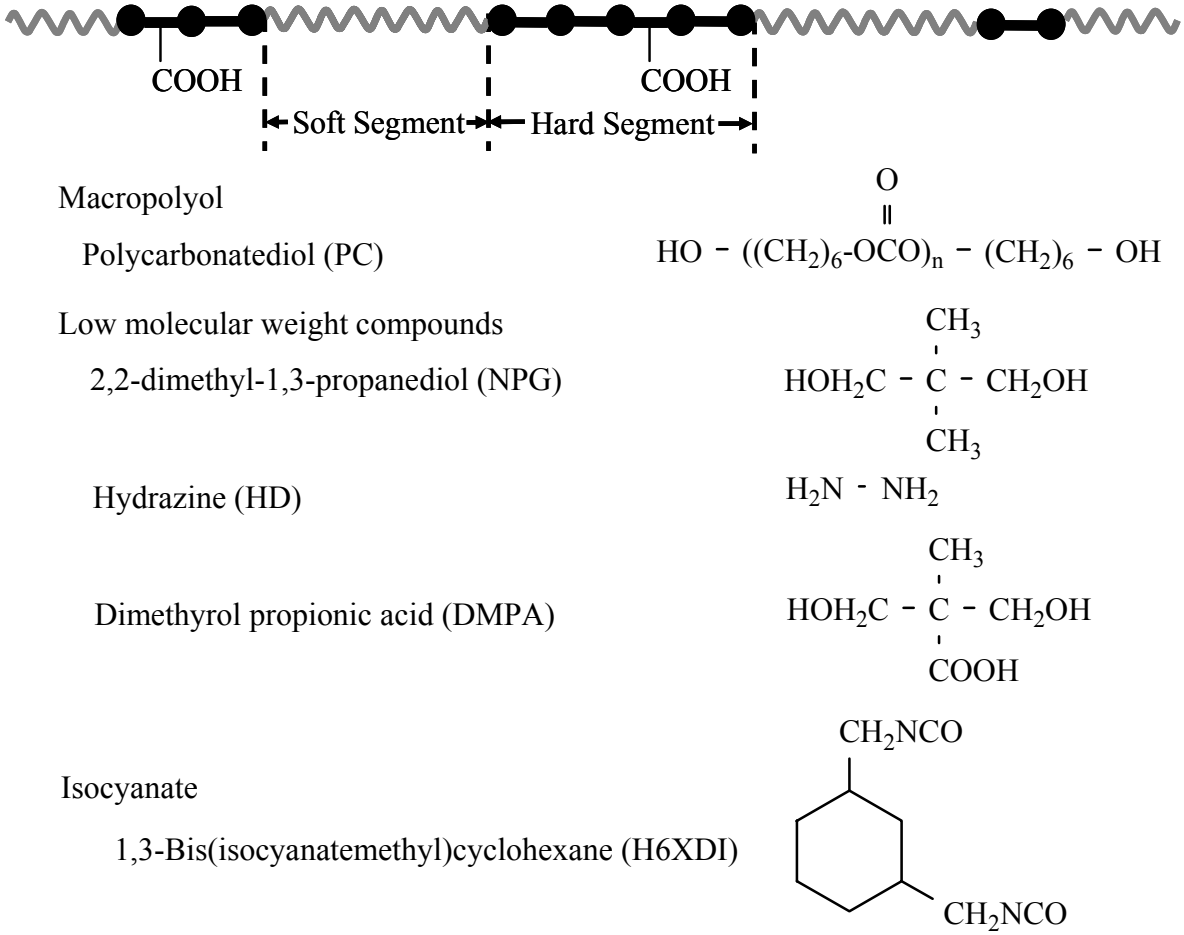

Figure 5-1. Schematic polyurethane-urea chain and starting compounds.

In this chapter, the role of the hard segment of PUD were investigated by using a few series of PUDs, which were prepared to have different distances and fractions of hard segments, the amount of ionic groups and the type of counterions. After examining the colloidal characteristics and the physical properties of these PUDs in relation to the chemical structures, the role of hard segments from the molecular side is discussed.

5.2. Experimental

5.2.1. Materials

Polycarbonate diol (PC) was dried under N_2 bubbling at 75 ˚C for 4 h. 2,2-Dimethyl-1,3-propanediol (NPG, Wako Pure Chemical Industries, Ltd.) was dried

under an N_2 atmosphere for more than 3 days. 1,3-Bis(isocyanatemethyl)cyclohexane (H6XDI, Mitsui-Takeda Chemical Industries, Ltd.), dimethylol propionic acid (DMPA), hydrazine monohydrate (HD, Wako Pure Chemical Industries, Ltd.), triethylamine (TEA, Wako Pure Chemical Industries, Ltd.), triisopropanolamine (TIPA, Wako Pure Chemical Industries, Ltd.), 2-dimethylaminoethanol (DMEA, Wako Pure Chemical Industries, Ltd.) and sodium hydrate (NaOH, Wako Pure Chemical Industries, Ltd.) were used without further purification.

5.2.2. Preparation of Aqueous Polyurethane-Urea Dispersion

PUD was prepared as follows. A 500 mL four-neck round-bottom flask equipped with a stirrer, a thermometer, a nitrogen inlet, and a condenser was charged with H6XDI (194.00 g, 1.0 mol) and acetonitrile (217.01 g) under nitrogen atmosphere. PC (Mn = 2,000, 246.91 g, 0.123 mol), NPG (25.73 g, 0.247 mol) and DMPA (39.70 g, 0.296 mol) were then added while stirring slowly, and the mixture was heated to 70 ˚C. They were allowed to react until the theoretical NCO content was detected by the dibuthylamine back-titration method (ASTM D 1638). The NCO-terminated prepolymer thus obtained was poured into an aqueous solution of tertially amines or NaOH as the neutralizing agent (counterions) under constant agitation (2,000 rpm). This dispersion was kept at 20 ˚C for 20 min to complete the neutralization reaction. DMEA, TEA, TIPA and NaOH were used as counterions. The stoichiometric ratio of counterions to COOH was 0.95. The neutralized NCO terminated polyurethane prepolymer was extended by adding a 10 % hydrazine monohydrate solution. The stoichiometric ratio of the amine group of hydrazine to NCO of the prepolymer was 0.95. The PUD (30 wt % concentration) was obtained by the evaporation of acetonitrile and then by adding an adequate amount of water. Table 5-1 shows the sample designation and composition. Samples were named

so that, for example in DM-20-2, the initial letter 'DM' refers to the counterion DMEA, 20 to the molecular weight 2000 of PC, and 2 to the COOH group weight content (%) in this polyurethane-urea dispersion.

5.2.3. Film Preparation

Film samples for mechanical and viscoelastic measurements were prepared by casting the dispersions on a metal plate. The films (about 0.1 mm thickness) were dried for longer than 1 day under ambient conditions to avoid producing foam or bubbles in the film at annealing. And then, the films were annealed at 130 ˚C for 1 h.

Table 5-1. The designation and composition (mol ratio) of aqueous polyurethane-urea dispersions (PUD).

PUD	Polymer composition (mol rario)				Counterion	COOH weight	Hard segment weight
	H6XDI	PC	NPG	DMPA	(0.95 eq.)	content (%)	fraction (%)
Series M							
DM-20-2	8.1	1	2	2.4	DMEA	2.6	52.6
DM-10-2	9.6	2	2	2.4	DMEA	2.4	55.8
DM-10-2H	8.1	1	2.6	1.8	DMEA	2.5	68.7
Series C							
DM-20-1	8.1	1	2.9	1.5	DMEA	1.6	52.3
DM-20-2	8.1	1	2	2.4	DMEA	2.6	52.6
DM-20-3	8.1	1	1	3.4	DMEA	3.6	52.9
Series N							
DM-20-2	8.1	1	2	2.4	DMEA	2.6	52.6
TE-20-2	8.1	1	2	2.4	TEA	2.6	52.6
TI-20-2	8.1	1	2	2.4	TIPA	2.6	52.6
Na-20-2	8.1	1	2	2.4	Na	2.6	52.6

The polyurethane prepolymer was prepared at NCO : OH =1.5 : 1 ratio. The PUD was prepared by the chain-extending reaction between NCO group of polyurethane prepolymer and NH_2 group of hydrazine monohydrate. The ratio of NCO group of polyuretahne prepolymer to NH_2 group of hydrazine monohydrate is 1 to 0.85.

5.2.4. Measurements

The average particle size was measured by light scattering (Coulter N4 Plus), where a He-Ne laser with a wavelength of 632.8 nm was used. The sample was diluted in deionized water to adjust the concentration for measurement.

Viscoelastic properties of films were measured at 10 Hz using a DVA-200 instrument (IT Keisokuseigyo) at a heating rate of 5 ˚C /min in the temperature range from -100 to 200 ˚C.

Mechanical properties were measured at 25 ˚C using INTESCO Model 205 following the ASTM D-412 specifications. A crosshead speed of 300 mm/min was used throughout these investigations to determine the ultimate tensile strength and elongation at break for all the samples. The values quoted are the average of five measurements.

5.3. Results and Discussion

5.3.1. Distance and Fraction of Hard Segment

In the polyurethane-urea molecule, the hard segment consists of urethane linkage generated by the reaction between H6XDI and low molecular weight diol or HD, and the soft segment is formed from macropolyol PC as shown in Figure 5-1. In a solid film, the hard segments aggregate by hydrogen bonding and form a hard domain. Therefore, the fraction of the hard segment in a polymer chain affects the number and the size of the hard domain. On the other hand, the length of soft segment, which is dependent on the PC molecular weight, determines the distance between the hard segments. In order to consider the influence of fraction and distance of the hard segments, three samples were prepared. Table 5-1 shows the specifications for these samples (Series M: DM-20-2, DM-10-2 and DM-10-2H). The length of the soft segment in DM-20-2 was different from that in DM-10-2, but the weight fraction of the hard segment was kept

constant by adjusting low molecular weight diols. Therefore, the mol ratio of PC in DM-10-2 was twice that in DM-20-2. In contrast, the mol ratio of PC to low molecular weight diol (NPG and DMPA) was kept constant for DM-20-2 and DM-10-2H, consequently increasing the weight fraction of the hard segment from 52.6 to 68.7. The last letter 'H' of DM-10-2H indicates that DM-10-2H has a larger hard segment fraction than the other samples. The differences of the three samples are schematically illustrated in Figure 5-2.

First, the colloidal characteristics of PUDs are discussed. Table 5-2 shows the particle sizes of the PUDs. By comparing the particle sizes of DM-20-2 and DM-10-2H, the particle size increases as the molecular weight of soft segment decreases. It is known that the ionic groups are located predominantly on the surface of particles and the ionomer dispersions are stabilized by the formation of electrical double layers. As the polyurethane chain becomes harder with decreasing length of soft segment, the formation of polymer micelles in water needs more chains to stabilize the micelle structure. In contrast with this result, the particle size decreased with the decrease of the

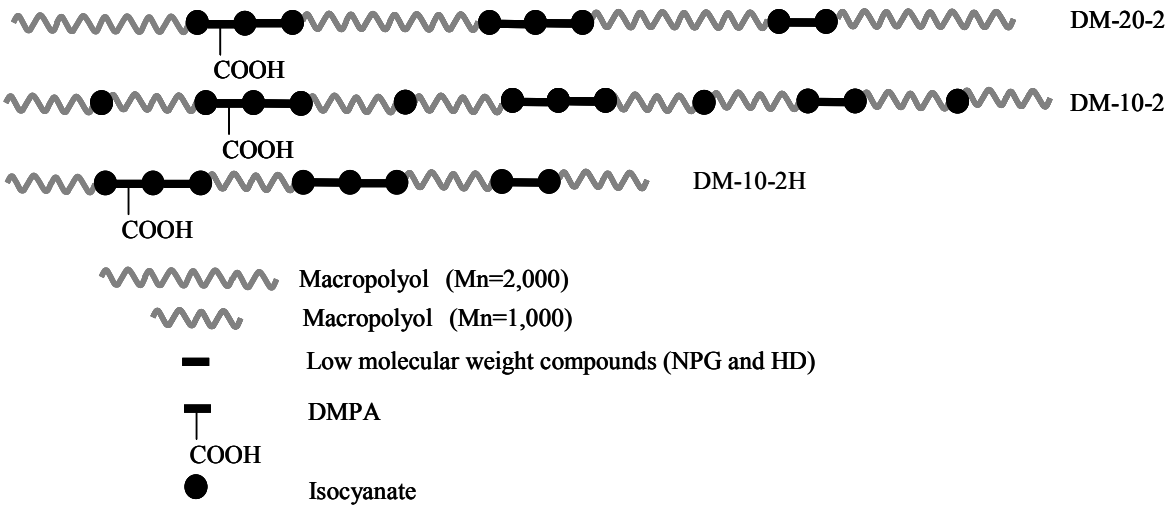

Figure 5-2. Illustration for the difference among three samples.

Table 5-2. The colloidal and physical properties of aqueous polyurethane-urea dispersions (PUDs).

Sample	Particle size (nm)	T_{gs} (℃)	T_{gh} (℃)	Tensile strength (MPa)	Young's modulus (MPa)	Strain at break (%)
Series M						
DM-20-2	55.7	-29.0	118	47.2	236	388
DM-10-2	23.0	-14.5	105	50.6	313	391
DM-10-2H	115.0	-7.0	122	57.2	388	17
Series C						
DM-20-1	99.2	-28.7	116	47.8	200	365
DM-20-2	55.7	-29.0	118	47.2	236	388
DM-20-3	44.1	-28.3	122	46.6	271	335
Series N						
DM-20-2	55.7	-29.0	118	47.2	236	388
TE-20-2	112	-28.5	108	43.7	296	386
TI-20-2	57.6	-28.0	108	40.4	229	373
Na-20-2	49.0	-28.5	130	52.0	210	390

soft segment length from DM-20-2 to DM-10-2 while the weight fraction of soft segment is fixed. This result was explained as an effect of homogeneous COOH group in a molecule. The smaller the molecular weight of PC is, the more uniformly the COOH group can be distributed. The uniform distribution of COOH group makes the formation of micelle easy, consequently the particle size becomes small.

In viscoelastic properties, there are large differences among the three samples, as shown in Figure 5-3. Table 5-2 shows the T_g values determined from the maxima of tan δ. Two peaks are observed in the tan δ curves. The lower temperature peak is considered as the glass transition temperature of the soft domains (T_{gs}) and the higher temperature peak is that of hard domains (T_{gh}). The comparison between DM-20-2 and DM-10-2 indicates that T_{gh} of DM-20-2 is higher than that of DM-10-2 and T_{gs} is opposite. These results can be explained as shown in Figure 5-4. Some hard segments existed in the soft domains and some soft segments existed in the hard domains, because the hard

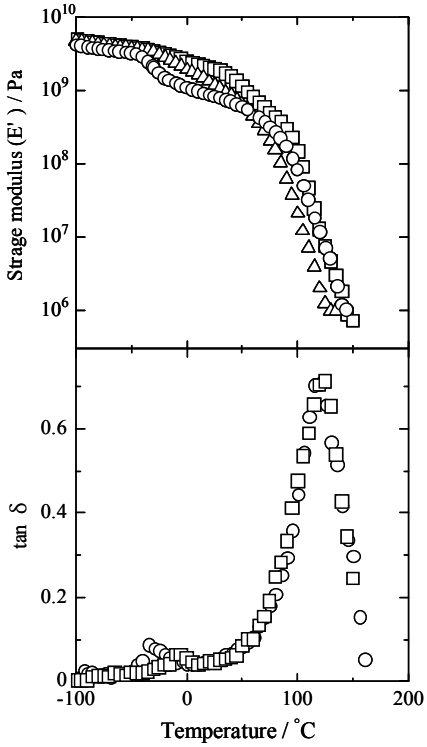

Figure 5-3. Storage Modulus (E') and tan δ for PUDs: (○) DM-20-2, (△) DM-10-2, (□) DM-10-2H.

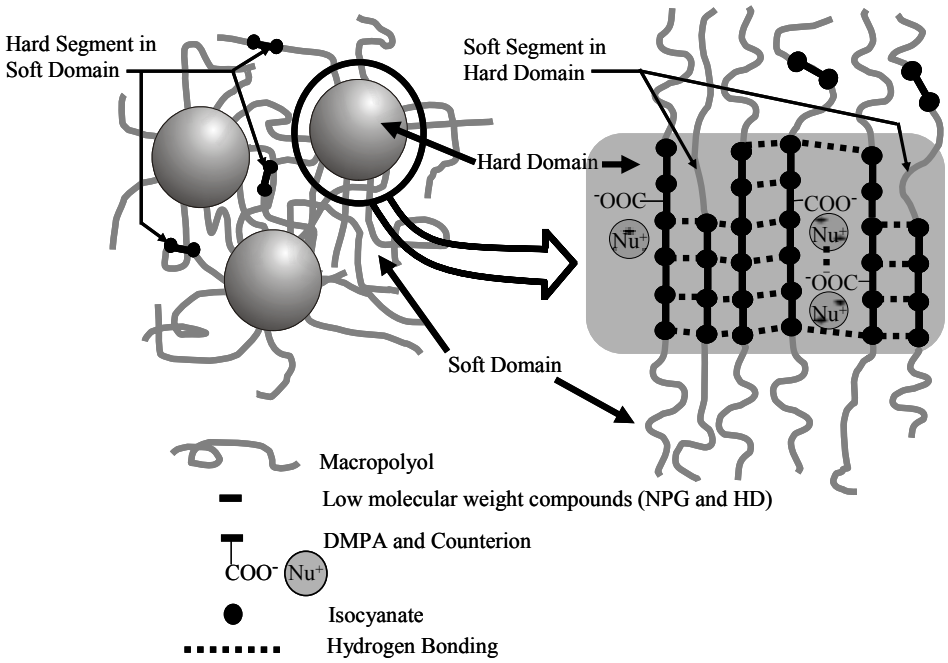

Figure 5-4. Schematic illustration for microphase separation structure of a film produced from the PUD.

segments were more uniformly distributed in DM-10-2 due to the short length of the soft segment. Therefore, T_{gs} increases under the influence of hard segments and T_{gh} decreases under the influence of soft segments.

DM-10-2H had the highest T_{gs} among the three samples due to the largest fraction of hard segments. It is interesting that T_{gs}s were quite different but T_{gh}s were almost the same at 120 ˚C for DM-20-2 and DM-10-2H. These results obtained on DM-20-2 show that there are few soft segments in the hard domains, and the phase separation proceeds almost completely both in the hard and soft domains.

Figure 5-5 and Table 5-2 show the mechanical properties of these three samples. DM-10-2H shows the most peculiar stress-strain curve of the three samples; the largest Young's modulus (388 MPa) and extremely small elongation are caused by the high fraction of hard segment in DM-10-2H. On the other hand, although the length of the

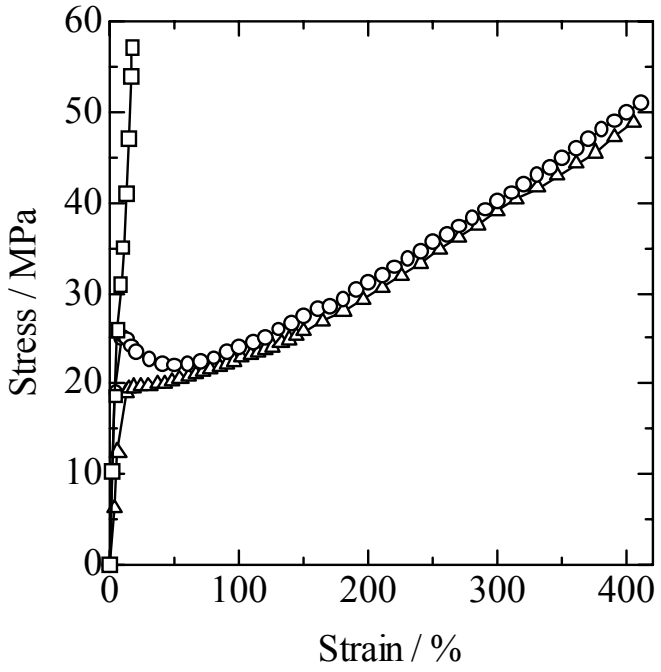

Figure 5-5. Stress-strain curves for PUDs:
(○) DM-20-2, (△) DM-10-2, (□) DM-10-2H.

soft segment is short in DM-10-2, it shows almost the same elongation as DM-20-2. This result shows that two PCs connected by urethane linkage, as shown in Figure 5-2, behave as a long chain of the soft segment to large deformation. However, the Young's modulus has a big difference between DM-10-2 (313 MPa) and DM-20-2 (236 MPa). This is the contribution of the hard segment of the urethane linkage connecting two PCs. Therefore, the hard segment has larger influence in minute deformation.

5.3.2. Amount of Ionic Compounds

In the previous section, the distance and the fraction of hard segments in a polyurethane chain were focused. In this section, the amount of ionic COOH group was changed in order to examine the cohesive force of the hard segment. The three samples of series C in Table 5-1 (DM-20-1, DM-20-2 and DM-20-3) were prepared to have COOH contents of 1.6, 2.6, or 3.6 wt % based on total solid. In colloidal characteristics, the particle size decreased with increasing COOH content, as shown in Table 5-2. Since the particle is stabilized by the hydrophilic groups in PUD, [8] it is natural for the particle size to become smaller as the COOH content increases.

Figure 5-6 shows the dynamic modulus and the stress-strain curves of three samples, and Table 5-2 shows T_{gh}s. As shown in Table 5-1, the hard segment fractions were almost the same among the three samples. Dynamic modulus, stress-strain curves and Young's modulus hardly changed among the three samples even when the content of hydrophilic DMPA increased. Only T_{gh} slightly rose with the increase of COOH content. These results show that microphase separation proceeds completely when the length of soft segment is long. Perhaps the COOH group contributes to promote microphase separation more strongly as compared with other nonionic species. However, in this experiment the condensed state of hard segments is not influenced by the COOH

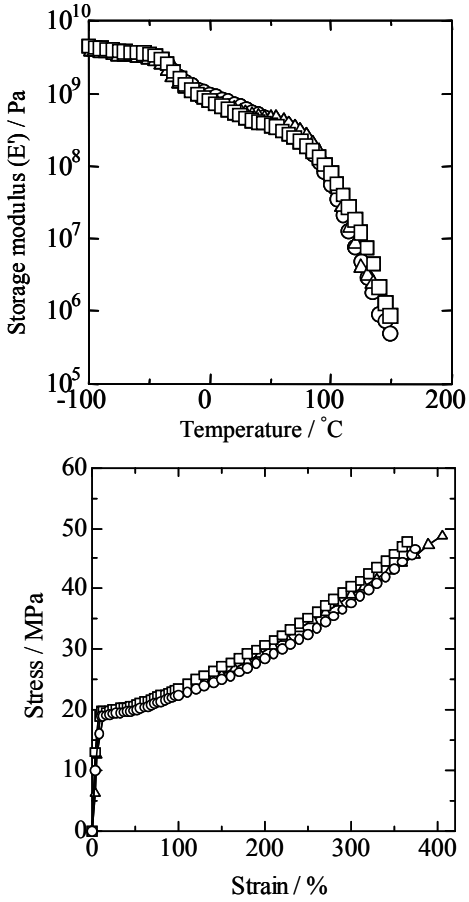

Figure 5-6. Storage modulus (E') and stress-strain curves for PUDs with different amount of COOH group: (○) DM-20-1, (△) DM-20-2 and (□) DM-20-3.

content, since microphase separation proceeds completely depending on the presence of long chain hydrophobic PC.

5.3.3. Type of Counterion

The type of counterion also affects the physical properties of PUDs. In this section, the series N in Table 5-1 are discussed. As to colloidal characteristics, TE-20-2 with the TEA counterion had a large particle size (112 nm) in comparison with the other dispersions with Na, DMEA and TIPA counterions. TEA has the weakest hydration ability among them because it has the hydrophobic ethylene group, but DMEA and

TIPA have the hydrophilic hydroxyl units. Na-20-2 showed the smallest particle size because it has the strongest hydration ability of metal cations among the four samples.

Figure 5-7 shows the tan δvalues and the stress-strain curves of N-series samples. T_{gs}s of four samples are almost the same, because the same PC was employed as the soft segment. On the other hand, T_{gh}s and mechanical properties were in the decreasing order of Na, DMEA, TEA and TIPA. These results indicate that counterions affect the condensed state of the hard segment. Assuming that the size of counterion is proportional to the molecular weight, their size increases in the order of Na (23), DMEA

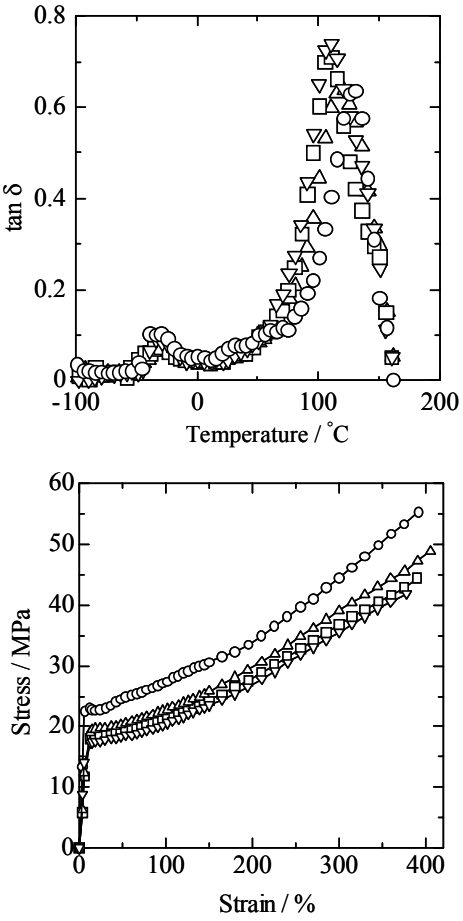

Figure 5-7. Tan δ and stress-strain curves for PUDs with different counterions: (○) Na-20-2, (△) DM-20-2, (□) TE-20-2 and (▽) TI-20-2

(89), TEA (101), and TIPA (192). This is consistent with the order of T_{gh}s, suggesting that the mechanical properties and Young's modulus are subjected to the plasticizing capacity of the counterion. It exists near the COOH group in the hard domains as shown in Figure 5-4, and the effect as a plasticizer in the hard domain becomes larger as its size becomes large, resulting in a weak cohesive force between the hard segments.

5.4. Conclusion

Differences in the fraction and distance of hard segments, the amount of COOH groups and the type of counterions appeared as the colloidal characteristics and physical properties of three series of PUDs.

The hard segment affected the colloidal characteristics of PUD. The increase in the fraction of hard segment enlarged the particle size of PUD micelles, because the polyurethane chain becomes harder with increasing fraction of hard segment and the formation of polymer micelles in water needs more chains to stabilize the micelle structure. Under a certain fraction of the hard segment, the homogeneous distribution of COOH group in the polyurethane chain resulted in a small particle size. The amount of COOH groups as hydrophilic unit also influenced the particle size of PUD, indicating that the larger amount of COOH groups led to the smaller particle size of PUD. Moreover, the hydrophilicity and hydration ability of the counterions affected the particle size of PUD.

In physical properties, the role of the hard segment was more important. The results of viscoelastic measurement showed that PUD had a microphase separation structure and two T_gs: T_{gh} derived from the hard domain and T_{gs} from the soft domain. The distance of the hard segments affected the microphase separation structure, resulting in an increase in T_{gs} and decrease in T_{gh} by the mutual penetration of the hard

and soft segments into the soft and hard domains with the reduction of the distance between the hard segments. In mechanical properties, the influence of the hard segment appeared most clearly in the Young's modulus. And the increase of the fraction of hard segment led to the high modulus and short elongation.

The component in hard segments, such as the amount of the COOH unit and the type of counterions, influenced the T_{gh}. The T_{gh} slightly rose with the increase of COOH content due to promotion of microphase separation by hydrogen bonding of the ionic COOH species. Furthermore, T_{gh} and Young's modulus were influenced by the plasticizing capacity proportional to the size of counterion.

These experimental results indicate that the detailed internal structure in the hard domain, as illustrated in Figure 5-4, is important knowledge for designing the chemical structure of PUDs.

References

1. S. Sakurai, Y. Okamoto, H. Sakaue, T. Nakamura, L. Banda and S. Nomura, *J. Polym. Sci., Part B: Polym. Phys*., **38**, 1716 (2000)
2. W. Tang, R. J. Farries, W. J. Macknight and C. D. Eisenbach, *Macromolecules*, **27**, 2814 (1994)
3. G. Consolati, M. Levi M and S. Turri, *Polymer*, **42**, 9723 (2001)
4. M. F. Sonnenschein, N. Rondan, B. L. Wendt and J. M. Cox, *J. Polym. Sci., Part A: Polym. Chem*., **42**, 2715. (2004)
5. D. J. Martin, G. F. Meijs, G. M. Renwick, S. J. Mccarthy and P. A. Gunatillake, *J. Appl. Polym. Sci*., **62**, 1377 (1996)
6. H. Tan, M. Guo, R. Du, X. Xie, J. Li, Y. Zhong and Q. Fu, *Polymer*, **45**, 1647 (2004)
7. L. F. Wang and Y. H. Wei, *Colloid and Surfaces B*, **41**, 249 (2005)
8. D. Dieterich, *Prog. Org. Coat*., **9**, 281 (1981)
9. S. Asaoka, T. Sakurai, M. Kitajima and H. Hanazawa, *J. Appl. Polym. Sci*., **73**, 741 (1999)
10. B. K. Kim and J. C. Lee, *J. Polym. Sci., Part A: Polym. Chem*., **34**, 1095 (1996)
11. S. Turri, M. Levi and T. Trombetta, *J. Appl. Polym. Sci*., **93**, 136 (2004)
12. Y. S. Kwak, S. W. Park, Y. H. Lee and H. D. Kim, *J. Appl. Polym. Sci*., **89**, 123 (2003)
13. T. Tawa and S. Ito, *Colloid Polym. Sci*., **283**, 731 (2005)
14. Y. M. Lee, J. C. Lee and B. K. Kim, *Polymer*, **35**, 1095 (1994)
15. D. J. Hourston, G. Williams, R. Satguru, J. D. Padget and D. Pears, *J. Appl. Polym. Sci.*, **66**, 2035 (1997)
16. D. J. Hourston, G. D. Williams, R. Satguru, J. C. Padget and D. Pears, *J. Appl.*

Polym. Sci., **74**, 556 (1999)

17. S. L. Hsu, H. X. Xiao, H. H. Szmant and K. C. Frisch, *J. Appl. Polym. Sci.*, **29**, 2467 (1984)
18. J. E. Yang, J. S. Kong, S. W. Park, D. J. Lee and H. D. Kim, *J. Appl. Polym. Sci.*, **86**, 2375 (2002)
19. D. C. Lee, R. A. Register, C. Z. Yang and S. L. Cooper, *Macromolecules*, **21**, 1005 (1988)
20. Y. Chen and Y. L. Chen, *J. Appl. Polym. Sci.*, **46**, 435 (1992)
21. S. A. Chen and J. S. Hsu, *Polymer*, **34**, 2769 (1993)
22. Y. S. Kwak, S. W. Park and H. D. Kim, *Colloid Polym. Sci.*, **281**, 957 (2003)
23. H. A. Al-salah, K. C. Frisch, H. X. Xiao and J. A. Mclean Jr., *J. Polym. Sci., Part A: Polym. Chem.*, **25**, 2127 (1987)
24. S. A. Chen and J. S. Hsu, *Polymer*, **34**, 2776 (1993)
25. B. K. Kim and J. C. Lee, *Polymer*, **37**, 469 (1996)
26. H. Xiao, H. X. Xiao, K. C. Frisch and N. Malwitz, *J. Appl. Polym. Sci.*, **54**, 1643 (1994)

Chapter 6

Gas Barrier Properties of Novel Type Aqueous Polyurethane-Urea Dispersion and Montmorillonite Composite

6.1. Introduction

In the field of food packaging, flexible films with a gas barrier function should be used to preserve the quality and freshness of many foods and beverages. Polymeric materials such as poly (ethylene terephthalate) (PET), polypropylene, nylon and polyethylene, widely used are gas-permeable; therefore polymer materials with oxygen barrier performance have been coated on the flexible packaging films. Structure and morphology of polymers which play key roles in retarding the permeation of gases through the polymer matrix have been investigated in order to attain the barrier performance. [1] Poly(vinylidene chloride) (PVDC) [2] and ethylene-vinyl alcohol copolymer (EVOH) [3, 4] are well-known coating materials with the lowest oxygen permeability. The barrier performance of them is due to the crystallinity and the structure packed by strong chain interaction of chlorine or hydroxyl units. However, the inadequate incineration of the materials including chloride compounds like PVDC causes an environmental problem of toxic dioxin emission. The oxygen barrier performance of EVOH drastically decreases in the presence of moisture. Consequently, it is strongly demanded to develop a new gas barrier coating material which does not contain chlorine molecules and does not depend on the humidity.

According to calculations by Salame, hydoroxyl and amide groups are effective on improving gas barrier property, because intermolecular cohesions by hydrogen bonding retard gas permeation.[5] Urethane and urea groups have high cohesion energy due to the strong hydrogen bonding. Therefore, the polyurethane-urea (PU) would provide high gas barrier property, but conventional PUs are known as a gas permeable polymer, because large amounts of the PU have a low concentration of urethane and urea groups due to the presence of soft segments. The soft segment is formed from polymer glycol so-called "macropolyol", and the hard segment is composed of the connection of diisocyanate and short chain diol or diamine with urethane or urea linkage. The increase of hard segment makes it hard to dissolve the PU into organic solvent. Aqueous polyurethane-urea dispersion (PUD) solves this problem. The form of dispersion allows the PU to have high concentration of urethane and urea groups.[6-14]

Further enhancement of gas barrier performance of polymers is achieved by dispersing small particles impermeable to gases.[15-19] Platelike nanoflakes are ideal due to their geometrical shape and high aspect ratio, and the effective improvement by introducing a small amount of them is important to retain the optical clarity mostly needed in packaging applications. Montmorillonite (MMT) is a representative material; however, there are only a few studies about the permeation-barrier properties of PU composites,[20-23] especially quite few about the PUD.

In this chapter, the novel type PUD with a high oxygen gas barrier property is prepared. It is the compositional characteristic that all components are hard segments. The relation between the gas barrier performance and the structure of PUD is examined from the molecular side. Further high level of the oxygen gas barrier property is achieved by the composition of PUD and MMT, and it strongly depends on the

distribution of MMT in PU matrix. The relation between the gas barrier performance and the structure of PUD-MMT composite is also discussed.

6.2. Experimental

6.2.1. Sample Preparation

Four PUD samples with different diol chain length were synthesized: ethylene glycol (EG: HO-C_2H_5-OH), diethylene glycol (DEG: HO-$(C_2H_5)_2$-OH), triethylene glycol (TEG: HO-$(C_2H_5)_3$-OH), and polycarbonatediol with molecular weight of 1000 (PC: HO-$((CH_2)_6$-$OCOO)_n$-$(CH_2)_6$-OH n=6-7, "T6001" Asahi Kasei Industries Ltd.). Table 6-1 shows the sample designation and composition. The PUD samples used in this chapter were synthesized as follows. First, the OH groups of diol including 2-2-bis(hydroxymethyl)propionic acid (DMPA, Nippon Kasei Chemical) were reacted with the NCO groups of 1,3-Diisocyanatomethyl cyclohexane (H6XDI, Mitsui

Table 6-1. The designation and composition (mol ratio) of PUD.

Reagent	PU-2	PU-4	PU-6	PU-40
H6XDI	0.86	0.81	0.76	0.76
DMPA	0.10	0.10	0.10	0.10
EG	0.38			0.29
DEG		0.35		
TEG			0.32	
PC				0.029
AEA	0.35	0.33	0.31	0.31
TEA	0.091	0.091	0.091	0.091
Urethane and Urea Content (mmol / g)	6.65	6.21	5.84	5.87

The polyurethane prepolymer was prepared at NCO : OH =1.8 : 1 ratio. The PUD was prepared by the chain-extending reaction between NCO group of polyurethane prepolymer and NH_2 group of AEA. The ratio of NCO group of polyuretahne prepolymer to NH_2 group of AEA is 1 to 0.92.

Samples were named so that, for example in PU-2, the letter '2' refers to the number of methylene unit of EG being the main diol to prepare PU-2.

Chemicals Polyurethanes, Inc.) in acetonitrile solution. After reaching the theoretical isocyanate content calculated from the ratio of H6XDI and diol, the obtained prepolymer containing carboxyl unit, H6XDI-diol-H6XDI, were neutralized with triethylamine (TEA, Wako Chemical). The neutralized prepolymer was poured into the distilled water under the constant agitation. At this stage, the stable aqueous dispersion is formed. Then, 2-(2-aminoethylamino)ethanol (AEA, Wako Chemical) was added into the prepolymer dispersion to conduct chain extension reaction. After that, the PUD was obtained by removing the residual acetonitrile in the rotary evaporation.

MMT "Kunipia-F" (10 g) purchased from Kunimine Co. was dispersed into distilled water (200 mL) with stirring at a room temperature and allowed to swell for 2 h. The MMT dispersion was placed for more than 1 day to swell completely. Before coating on the substrate, the required amount of the MMT dispersion was added to the PUD with stirring for 30 min at a room temperature and then the mixture was left for 1 h.

For the fluorescence measurement, the MMT labeled by fluorescent dye, rhodamine B (RhB), was used. The fluorescence label of MMT was performed in the following manner. [24, 25] An aqueous solution of RhB (Wako Chemical) at a concentration of 60 mM, and then 500 mg of MMT was added to the RhB solution. RhB was adsorbed for 7 days at a room temperature. The dye-labeled MMT was separated as a precipitate by centrifugation (750 g, 20 min). The upper solution was clear and colorless; therefore, RhB was estimated to be completely adsorbed by MMT. The dye-labeled MMT and pure MMT was blended by the weight ratio = 1 : 100. The dispersion of MMT in the PUD matrix was observed by fluorescence microscopy.

PUD and PUD-MMT composite was coated with a bar coater on the polyethylene

terephthalate (PET) film (15 μm thick) with corona-treated surfaces. PET film "Lumirror P60" was purchased from Toray Co. The film was dried at 90 ˚C for 2 min immediately after coating and then it was left for more than 1 day under an ambient atmosphere. The thickness of the coating layer was ca. 2 μm.

6.2.2. Measurements

The oxygen transmission rate (OTR) through a PET film coated with the PUD or the PUD-MMT composite was measured by an OX-TRAN2 (Mocon, Minneeapolis, MN) at 23 ˚C, 1 atm and 80 % RH. The OTR was normalized with respect to the film thickness. The transmission rate through the PUD or PUD-MMT composite layer was calculated by deducting the contribution of the plane PET film.[26] An average of three measurements for each sample is reported.

The morphology of the film formed from the PUD-MMT composite was observed by a fluorescence microscope (NIKON ECLIPSE TE2000-E) at 23 ˚C, 50 % RH.

6.3. Results and Discussion

6.3.1. PUD with Gas Barrier Performance

Figure 6-1 shows the OTR of the coating layer formed from PUD. PU-40 is the conventional PUD consisting of the soft and hard segments, and PU-2, PU-4, and PU-6 are the novel type PUDs consisting of only hard segment. The difference between PU-40 and PU-6 is due to the existence of macropolyol in the PU backborne, although both samples have almost the same content of the urethane and urea groups of 5.9 mmol / g. The high OTR value of PU-40 compared to that of PU-6 indicates that the macropolyol in PU molecule, the soft segment, decreases the oxygen barrier

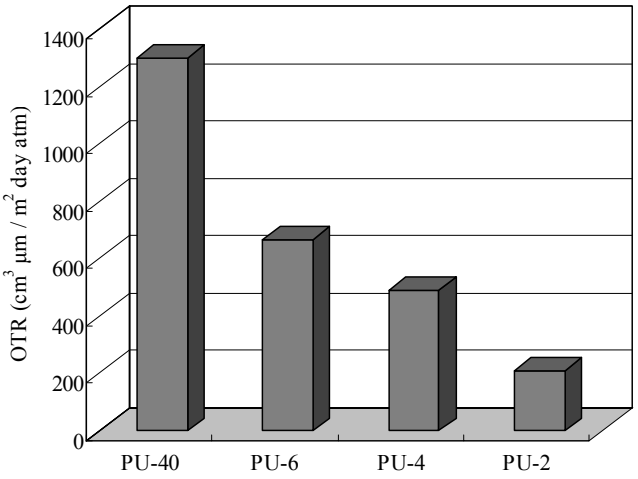

Figure 6-1. Oxygen transmission rates (OTR) of conventional (PU-40) and novel type (PU-2, PU-4, and PU-6) of PUD.

performance. As schematically shown in Figure 6-2, PU-6 has only hard segments. In the hard segment domain, the PU chain is closely packed due to the strong interaction among the urethane and urea groups. On the other hand, PU-40 has the microphase separation structure of the soft and hard segment domains in the film. The PC in the soft segment domain is a flexible chain without a cohesive functional group. Consequently, there is much free space to pass gas molecules.

The comparison of the OTR values among PU-6, PU-4, and PU-2 shows the effect of the structure of the hard segment at a molecular level on oxygen barrier performance. The difference among three samples is the chain length of diol composed of the hard segment. The chain length determines the distance between urethane or urea groups, that is, the increase of the chain length of diol results in the decrease of the concentration of urethane and urea group as illustrated in Figure 6-2. The increase of their groups makes the hard domains stiffer due to the hydrogen bondings. The stiff hard

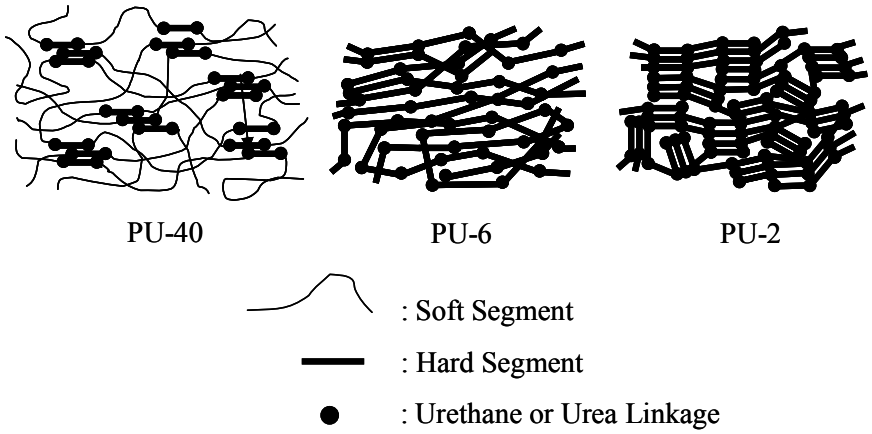

Figure 6-2. Schematic illustration of the structure difference of conventional and novel type PUD.

domains serve as the retardation of the oxygen gas permeation. Consequently, the increase of urethane and urea groups improves the oxygen barrier property.

The lack of macropolyol in PU molecule brings about the weakness of the obtained film. However, the defect is covered by the extremely high concentration of urethane or urea linkages, which provide properties of both physical crosslinkage and filler-like reinforcement due to the intermolecular hydrogen bonding. Therefore, the novel type PUD attains the balance of the flexibility and the hardness.

6.3.2. PUD-MMT Composite

In order to improve the gas barrier performance, it is an effective method to distribute inorganic compounds like MMT in a polymer matrix, because an impermeable inorganic compound physically disturbs the gas permeation. The OTR of PU-40 is improved from 1300 ($cm^3 \cdot \mu m / m^2 \cdot day \cdot atm$) to 500 ($cm^3 \cdot \mu m / m^2 \cdot day \cdot atm$) by the addition of MMT with 4.9 vol %. However, the OTR value is inferior to that of PVDC (100 $cm^3 \cdot \mu m / m^2 \cdot day \cdot atm$), which is a representative polymer with the highest

gas barrier property. The improvement of gas barrier property is expectable by distributing MMT into the novel type PUD. So, the OTR value of the composite of PU-2 and MMT was examined. The closed circles in Figure 6-3 show the OTR for the composite film with 2 μm thickness as a function of the MMT volume fraction. The OTR decreased with increasing the MMT volume fraction; the reduction of 70 % in permeability was attained at a MMT volume fraction of 4 %. The reduction in OTR is obviously a consequence of the long tortuous path that the oxygen molecules have to penetrate the composite film.

There is a lot of literature to discuss the transport of solutes in a polymer composite [15-19]. The theory of Gusev et al. [16] employs circular disks of diameter, *d*, and thickness, *t*.

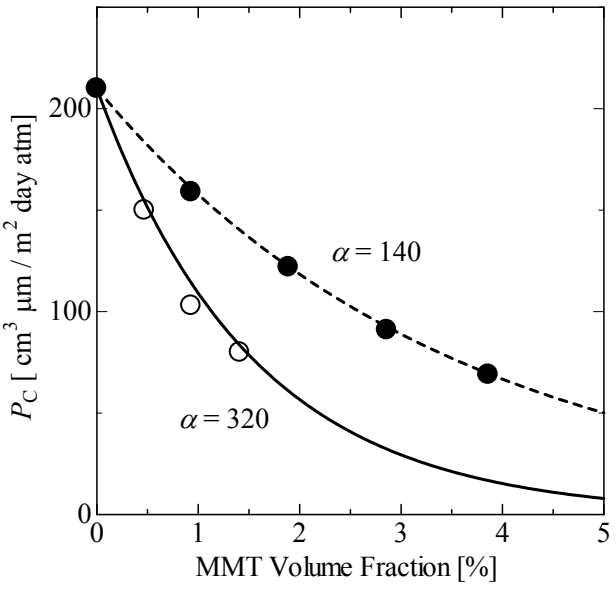

Figure 6-3. Oxygen transmission rate for the PUD-MMT composites as a function of MMT content with different film thickness: closed circle; 2.0 μm, open circle: 0.4 μm. The dashed and solid lines represent the calculated value from Gusev's equation for α = 140 and 320, respectively.

The aspect ratio, α, is defined as $\alpha = d/t$. The theory allows for random placement of disks in space with the orientation parallel to the film plane. Gusev et al. found that the gas permeability (P_c) through the thickness of a composite film could be represented by the stretched exponential function as following.

$$P_C = \frac{P_0}{\exp(\alpha\phi/3.47)^{0.71}}$$

P_0 is the gas permeability of a polymer, ϕ is the volume fraction of impermeable flakes. The dashed line in Figure 6-3 represents the calculated value on the assumption of α = 140 for the permeability through the composite. The curve calculated from the theoretical model is well fitted with the experimental data. However, the value of α = 140 is small, considering the thickness of the individual MMT layers (1 nm).[27] The small value is considered because the distribution and orientation of the MMT in PU matrix influences the gas barrier property.

Figure 6-4 shows the fluorescent micrograph of the PUD-MMT composite containing MMT at 0.93 vol. %. From the micrograph, it was found that the MMTs

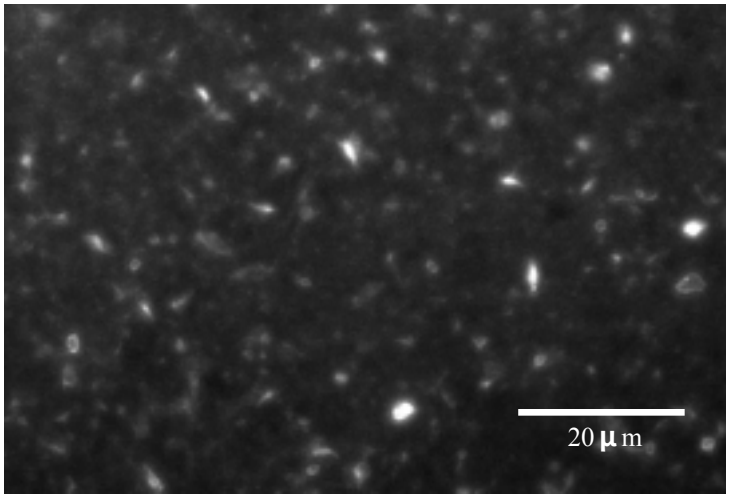

Figure 6-4. Fluorescence micrograph of the PUD-MMT composite; MMT volume fraction is 0.92 %.

were uniformly dispersed in the PU matrix and the size of MMT was ca. 2 μm. The size of MMT is important, because MMTs are able to take various directions in polymer matrix at a larger film thickness than their own sizes. Open circles in Figure 6-3 show the experimental OTR values when PUD-MMT composite is coated at 0.4 μm film thickness and then PUD is overcoated at 1.6 μm film thickness. The volume fraction was calculated from a quantity of MMT to the total amount of PUD. The OTR values in the thin film coatings were remarkably small. The reason for this is illustrated in Figure 6-5. At 2.0 μm film thickness, MMTs disperse at various direction in PU matrix. However, the direction of MMT is restricted at 0.4 μm film thickness, because the size of MMT is ca. 2.0 μm. The solid line in Figure 6-3 represents the calculated value on the assumption of α = 320 for the permeability through the composite. The increase of the value of α suggests that the MMT has to be aligned parallel to the substrate in the thin film thickness. The parallel arrangement of the MMT in PU matrix is effective in disturbing the permeation of the gases. Therefore, thin film coating of the PUD-MMT composite achieves the high gas barrier performance.

6.4. Conclusion

The novel type PUD with oxygen barrier performance was prepared. The

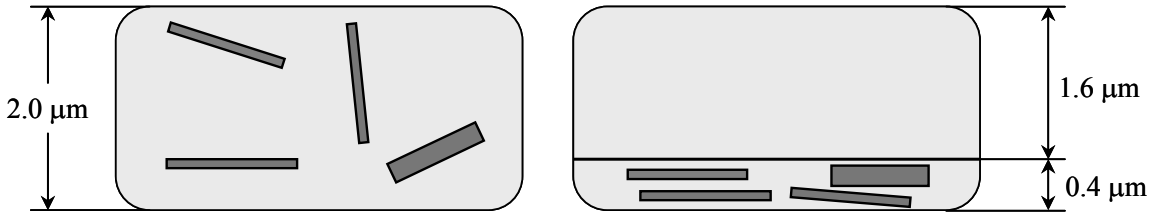

Figure 6-5. Schematic illustration of the structure of PUD-MMT composites with different film thickness.

characteristic molecular structure consisting of only hard segments and the extremely high concentration of the urethane and urea group were important to achieve the high oxygen barrier property. And the increase of urethane and urea groups in the hard segment improved oxygen barrier performance since the firmly packed hard domains by the hydrogen bonding retarded the oxygen gas permeation.

In PUD-MMT composite, the fluorescent micrograph showed that MMT with the size of ca. 2 μm dispersed in PU matrix uniformly. The alignment of MMT in PU matrix influenced the oxygen barrier property considerably. The OTR was improved by changing the film thickness of PUD-MMT composite from 2.0 μm to 0.4 μm. This is because the MMT with the size of ca. 2.0 μm had to be aligned parallel to the substrate at 0.4 μm film thickness, due to the geometric restrictions.

The composition of the novel type PUD and the MMT achieved the oxygen barrier property higher than PVDC. The gas barrier property is not dependent on humidity like EVOH. Since the PUD-MMT composite films do not contain chlorine and attain the reduction of volatile organic compounds, they are completely new eco-friendly coating materials with high oxygen barrier property.

References

1. M. Salame, *J. Plast. Film Sheeting,* **2**, 321 (1986)

2. P. T. DeLassus, *J. Vinyl Technol.*, **1**(1), 14 (1979)

3. J. A. Wachtel, B. C. Tsai, and C. J. Farrell, *Plast. Eng*., **2**, 41 (1985)

4. B. C. Tsai, and B. J. Jenkins, *J. Plast. Film Sheeting*, **4**, 63 (1988)

5. M. Salame, *Polym. Eng. Sci.*, **26**, 1543 (1986)

6. D. Dieterich, *Prog. Org. Coat*., **9**, 281 (1981)

7. H. A. Al-salah, K. C. Frisch, H. X. Xiao and J. A. Mclean Jr., *J. Polym. Sci, Part A: Polym. Chem.*, **25**, 2127 (1987)

8. K. L. Noble, Prog. Org. Coat., **32**, 131 (1997)

9. B. K. Kim, and J. C. Lee, *J. Polym. Sci. Part A: Polym. Chem.*, **34**, 1095 (1996)

10. M. Melchiors, M. Sonntag, C. Kobusch, and E. Jürgens, *Prog. Org. Coat.*, **40**, 999 (2000).

11. Z. W. Wicks, Jr., D. A. Wicks, and J. W. Rosthauser, *Prog. Org. Coat* ., **44**, 161 (2002)

12. T. Tawa, and S. Ito, *Colloid Polym. Sci.*, **283**, 731 (2005)

13. T. Tawa, and S. Ito, *Polym. J.*, **38**, 686 (2006)

14. A. K. Nanda, and D. A. Wicks, *Polymer*, **47**, 1805 (2006)

15. G. H. Fredrickson, and J. J. Bicerano, *J. Chem. Phys.*, **110**, 2181 (1999)

16. A. A. Gusev, and H. R. Lusti, *Adv. Mater.*, **13**, 1641 (2001)

17. L. E. Nielsen, *J. Macromol. Sci., (Chem.)*, **A1**, 929 (1967)

18. N. K. Lape, E. E. Nuxxoll, and E. L. Cussler, *J. Membr. Sci.*, **236**, 29 (2004)

19. C. Yang, W. H. Smyrl, and E. L. Cussler, *J. Membr. Sci.*, **231**, 1 (2004)

20. R. Xu, E. Manias, and A. J. Snyder, *Macromolecules*, **34**, 337 (2001)

21. J. H. Chang, and Y. U. An, J. Appl. Polym. Sci. Polym. Chem., **40**, 670 (2002)

22. M. Tortora, G. Gorrasi, V. Vittoria, G. Galli, S. Ritrovati, and E. Chiellini, *Polymer*, **43**, 6147 (2002)

23. M. A. Osman, V. Mittal, M. Morbidelli, and U. W. Suter, *Macromolecules*, **36**, 9851 (2003)

24. F. L. Arbeloa F. L. J. M. H. Martinez, T. L. Arbeloa, and I. L. Arbeloa, *Langmuir*, **14**, 4566 (1998)

25. T. Endo, N. Nakada, T. Sato and M. Shimada, *J. Phys. Chem. Sol.*, **49**, 1423 (1988)

26. J. Crank, *The Mathematics of Diffusion; Clarendon Press: Oxford, England*, (1998)

27. E. P. Giannelis, *Adv. Mater.*, **8**, 29 (1996)

Summary

This thesis described the characteristics and properties water dispersible polyisocyanate (WDPI) and polyurethane dispersion (PUD). Part I in this thesis focuses on the reaction and structural change of the WDPI micelle and the mechanical properties of the obtained film with the reaction of NCO groups. Part II clarified the effect of hard segment in PUD on physical properties of the film. A summary of each chapter is presented below.

In Chapter 2, a novel WDPI was synthesized by the reaction of the allophanate of hexamethylene diisocyanate with MPEG. This WDPI had a very low viscosity and formed stable aqueous dispersion by simply mixing method. The WDPI showed the distinctive reaction behavior in water medium with an induction period. The induction period was closely related to the particle diameter of WDPI micelle. The diameter became small with the content of the hydrophilic MPEG, resulting in the short induction period. The feature of the reaction was a stepwise with the elapse of time. This is because the WDPI forms the micelle with core-shell structure in aqueous medium and the reaction depends on the location of the reaction inside the micelles.

Chapter 3 described the structure change inside the WDPI micelle with the reaction in aqueous medium, which was probed by the microviscosity of the micelle. The microviscosity was quantitatively estimated by the two fluorescence techniques; the excimer formation rate and the fluorescence depolarization revealed the translational and rotational diffusivities in the interior of micelles, respectively. The fluorescent dyes existed in the core of the WDPI micelle locally due to their hydrophobicities. Therefore,

they reflected the internal state of the WDPI micelle. The microviscosity change of the WDPI micelle showed that the NCO groups of the WDPI were retained in the core of micelles during the induction period, and the sudden polymerization after the induction period led to the drastic increase of microviscosity of WDPI micelle. These results indicated that the microviscosity of the individual micelle and the practical performance of the waterborne coating system had a close relation.

In Chapter 4, the intermicellar reaction in the waterborne two-component polyurethane (WB 2K-PU) system was examined. In WB 2K-PU system, the reaction between PUD and WDPI proceeded preferentially in the colloidal state due to the advantageous location and the high reactivity of the OH groups of PUD. The film morphology was drastically changed with time after mixing of WDPI and PUD. The changes were mainly caused by the increase of the high molecular weight compounds produced by the intermolecular reaction between PUD and WDPI. They aggregated and formed the phase separated structure because of the incompatibility due to the outstanding high molecular weight, resulting in the decrease of the mechanical strength of the obtained film.

In Chapter 5, the influence of hard segment of PUD on the colloidal characteristics and physical properties of the obtained film were studied. The colloidal characteristics of PUD were affected by the hard segment. The increase in the fraction of hard segment enlarged the particle size of PUD micelles, because the polyurethane chain becomes harder with increasing fraction of hard segment and the formation of polymer micelles in water needs more chains to stabilize the micelle structure. Under a certain fraction of the hard segment, the homogeneous distribution of COOH group in the PU chain resulted in a small particle size. In physical properties, the role of the hard

segment was more important. The results of viscoelastic measurement showed that the film obtained from PUD had a microphase separation structure with two T_gs: T_{gh} from the hard domain and T_{gs} from the soft domain. The distance of the hard segments affected the microphase separation structure, resulting in an increase in T_{gs} and decrease in T_{gh} by the mutual penetration of the hard and soft segments into the soft and hard domains with the reduction of the distance between the hard segments. The increase of the fraction of hard segment led to the high modulus and short elongation in mechanical property.

In Chapter 6, the structure of PUD was discussed in order to achieve oxygen barrier property. A novel type PUD was prepared, of which the characteristic molecular structure was in the extremely high concentration of the urethane and urea group, and all components were considered as hard segments. Generally, the microphase separation structure of a conventional PU leads disadvantage in gas barrier performance, because the soft domain works as the pathway of gas. However, the novel type PUD does not have a soft segment, and the increase of urethane and urea groups improved oxygen barrier performance. The oxygen barrier property of the composite of the novel PUD and montmorillonite (MMT) was also examined. In PUD-MMT composite, the distribution of MMT in PU matrix is important for improving the oxygen barrier property. The structure that the MMT in PU matrix was arranged in parallel to the substrate was effective in improvement of gas barrier property. The composite does not contain chlorine. It may serve as an eco-friendly coating materials with gas barrier property.

List of Publications

Chapter 2

"Preparation and Reactions of Hydrophilic Isocyanate Micelles Dispersed in Water"
Tsutomu Tawa and Shinzaburo Ito

Colloid and Polymer Science, **283**, 731-737 (2005).

Chapter 3

"Microviscosity of the Reactive Water-Dispersible Polyisocyanate Micelle as Studied by Fluorescence Probe Techniques"

Tsutomu Tawa, Hiroyuki Aoki, and Shinzaburo Ito

Journal of Applied Polymer Science, submitted.

Chapter 4

"Colloidal Characteristics and Film Properties of Waterborne Two-component Polyurethanes"

Tsutomu Tawa, Hiroyuki Aoki, and Shinzaburo Ito

Colloid and Polymer Science, submitted.

Chapter 5

"The Role of Hard Segments of Aqueous Polyurethane-urea Dispersion in Determining the Colloidal Characteristics and Physical Properties"

Tsutomu Tawa and Shinzaburo Ito

Polymer Journal, **38**, 686-693 (2006).

Chapter 6

"Gas Barrier Properties of Novel Type Aqueous Polyurethane Dispersion and Montmorillonite Composite"

Tsutomu Tawa, Hiroyuki Aoki, Takatsugu Kito, Yoshiumi Kohno,
Ryoka Matsushima, and Shinzaburo Ito

In preparation.

Others

"Kinetic Analysis of Triplet Energy Migration in Poly[(2-naphthylalkyl methacrylate)-*co*-(methyl methacrylate)]s and Poly[(9-phenanthrylmethyl methacrylate)-*co*-(methyl methacrylate)] Solid Films"

Hideaki Katayama, Tsutomu Tawa, Gregory W. Haggquist, Shinzaburo Ito, and Masahide Yamamoto

Macromolecules, **26**, 1265-1269 (1993).

"Intramolecular Triplet Energy Migration in Poly(2-vinylnaphthalene) and Poly(naphthylalkyl methacrylate)s in Solid Solution: Effects of Side Chain Length"

Hideaki Katayama, Tsutomu Tawa, Shinzaburo Ito, Masahide Yamamoto, and Yoshio Wada

Polymer Bulletins, **29**, 365-367 (1992).

"Interchromophore Interaction of the Excited Triplet-state in Poly(naphthylalkyl methacrylate) Copolymer Films"

Hideaki Katayama, Tsutomu Tawa, Shinzaburo Ito, and Masahide Yamamoto

Journal of the Chemical Society-Faraday Transactions, **88 (18)**, 2743-2746 (1992).

"Studys on Aqueous Polyurethane Dispersion"

Tsutomu Tawa, and Takashi Uchida

Toso Kougaku, **42 (2)**, 62-68 (2007).

Patents

Japanese Patent 3351574
Tsutomu Tawa, Teruo Hori, and Kyuya Yamazaki

Japanese Patent 3524911
Tsutomu Tawa, Teruo Hori, and Kyuya Yamazaki

Japanese Patent 3872969
Youichiro Mori, Ryou Yoshida, Hiroshi Kanai, Akihiro Miyasaka, Tsutomu Tawa, Chikako Kouda, and Mitsuhiro Nishimura

Japanese Patent 3970955
Tsutomu Tawa, and Teruo Hori

Japanese Patent H07-010950
Tsutomu Tawa, Teruo Hori, and Kyuya Yamazaki

Japanese Patent H08-183829
Tsutomu Tawa, Sachio Igarashi, and Kyuya Yamazaki

Japanese Patent H09-012864
Tsutomu Tawa, and Teruo Hori

Japanese Patent 2000-102764
Tsutomu Tawa, Chikako Kouda, Fumiaki Hirata, Youichiro Mori, Makoto Yamazaki, and Hidetoshi Shinto

Japanese Patent 2000-102765
Tsutomu Tawa, Chikako Kouda, Fumiaki Hirata, Youichiro Mori, Makoto Yamazaki, and Hidetoshi Shinto

Japanese Patent 2000-178880
Chikako Kouda, Tsutomu Tawa, and Fumiaki Hirata

Japanese Patent 2000-309747
Youichiro Mori, Makoto Yamazaki, Masahiro Fuda, Ryousuke Wake, Tsutomu Tawa, Chikako Kouda, and Fumiaki Hirata

Japanese Patent 2001-019902
Youichiro Mori, Tatsuya Sakiyama, Masahiro Fuda, Ryousuke Wake, Masao Kurosaki, Teruaki Isaki, Tsutomu Tawa, Chikako Kouda, and Fumiaki Hirata

Japanese Patent 2001-342577
Youichiro Mori, Shiro Fujii, Yuichi Sato, Ken Takada, Tsutomu Tawa, and Fumiaki Hirata

Japanese Patent 2002-120323
Youichiro Mori, Akihiro Miyasaka, Hiroshi Kanai, Ikuro Yamaoka, Tsutomu Tawa, Chikako Kouda, and Mitsuhiro Nishimura

Japanese Patent 2002-060971
Youichiro Mori, Hiroshi Kanai, Ikuro Yamaoka, Tsutomu Tawa, Chikako Kouda, and Mitsuhiro Nishimura

Japanese Patent 2002-144478
Ikuro Yamaoka, Hiroshi Kanai, Akihiro Miyasaka, Youichiro Mori, Tsutomu Tawa, Mitsuhiro Nishimura and Chikako Kouda

Japanese Patent 2002-363525
Tsutomu Tawa, Teruo Hori, and Kyuya Yamazaki

Japanese Patent 2003-003278
Ikuro Yamaoka, Youichiro Mori, Hiroshi Kanai, Tsutomu Tawa, Chikako Kouda, and Mitsuhiro Nishimura

Japanese Patent 2003-027256
Ikuro Yamaoka, Youichiro Mori, Hiroshi Kanai, Akihoro Miyasaka, Tsutomu Tawa, Chikako Kouda, and Mitsuhiro Nishimura

Japanese Patent 2003-062927
Youichiro Mori, Ryo Yoshida, Hiroshi Kanai, Akihoro Miyasaka, Tsutomu Tawa, Chikako Kouda, and Mitsuhiro Nishimura

Japanese Patent 2005-139435
Takashi Uchida, Tsutomu Tawa, and Hiroyuki Shiraki

Japanese Patent 2005-139436
Takashi Uchida, Tsutomu Tawa, and Takuzo Imaizumi

U. S. Patent 6569533
Takashi Uchida, Tsutomu Tawa, and Hiroyuki Shiraki

U. S. Patent 6979493
Takashi Uchida, Tsutomu Tawa, and Hiroyuki Shiraki

Acknowledgments

The study presented in this thesis was carried out at the Department of Polymer Chemistry, Graduate School of Engineering, Kyoto University, from 2002 to 2008, under the guidance of Professor Shinzaburo Ito. The author sincerely expresses gratitude to Professor Shinzaburo Ito for his continuous guidance, valuable advices, and significant discussions throughout this study. The author makes a most cordial acknowledgement to Professor Shinzaburo Ito, again.

The author is sincerely indebted to Associate Professor Hiroyuki Aoki for his kind guidance and thoughtful advice. The author has received directly his research guidance and significant advice.

The author is most grateful to Associate Professor Hideo Ohkita and Dr. Masataka Ohoka for their suggestion and advice in various situations.

The author is profoundly grateful to Mr. Takashi Uchida in Mitsui Chemicals Polyurethanes, Inc. for providing the valuable samples and helpful advice especially in the study of a novel type polyurethane with oxygen barrier performance.

The author acknowledges the active collaboration and helpful discussion with the previous and present colleagues of Ito Laboratory: especially, Dr. Toshiki Fushimi, Dr. Hiroaki Benten, and Mr. Rhosyun Sekine. Without their collaboration and support, the author could not carry out his studies.

At last, the author expresses his sincere gratitude to his wife Keiko Tawa and his son Yuuki Tawa, for their continuous support and encouragement.

January, 2008

Tsutomu Tawa